Preprints.org

Article

Not peer-reviewed version

Antibacterial Effects of Sulfated Chitosan Against *Piscirickettsia salmonis*: A Biomimetic Strategy as an Antimicrobial Alternative in Aquaculture for Cell Membrane Disruption and Antibiofilm Activity

Darwuin Arrieta-Mendoza , Alejandro A. Hidalgo , Andrónico Neira-Carrillo * , Sergio A. Bucarey *

Posted Date: 1 April 2026

doi: 10.20944/preprints202604.0022.v1

Keywords: sulfated chitosan; *Piscirickettsia salmonis*; antibiofilm activity; antibacterial effect; antimicrobial alternative; heparan sulfate mimetic; bacterial membrane disruption

Preprints.org is a free multidisciplinary platform providing preprint service that is dedicated to making early versions of research outputs permanently available and citable. Preprints posted at Preprints.org appear in Web of Science, Crossref, Google Scholar, Scilit, Europe PMC.

Copyright: This open access article is published under a Creative Commons CC BY 4.0 license, which permit the free download, distribution, and reuse, provided that the author and preprint are cited in any reuse.

Preprints.org (www.preprints.org) | NOT PEER-REVIEWED | Posted: 1 April 2026 doi:10.20944/preprints202604.0022.v1

Disclaimer/Publisher's Note: The statements, opinions, and data contained in all publications are solely those of the individual author(s) and contributor(s) and not of MDPI and/or the editor(s). MDPI and/or the editor(s) disclaim responsibility for any injury to people or property resulting from any ideas, methods, instructions, or products referred to in the content.

Article

Antibacterial Effects of Sulfated Chitosan Against *Piscirickettsia salmonis*: A Biomimetic Strategy as an Antimicrobial Alternative in Aquaculture for Cell Membrane Disruption and Antibiofilm Activity

Darwuin Arrieta-Mendoza [1,2], Alejandro A. Hidalgo [3], Andrónico Neira-Carrillo [4,*] and Sergio A. Bucarey [1,*]

[1] Centro Biotecnológico Veterinario, Biovetec. Departamento de Ciencias Biológicas, Facultad de Ciencias Veterinarias y Pecuarias, Universidad de Chile. Santa Rosa 11735, La Pintana, Santiago, Chile

[2] Doctoral Program in Agricultural and Veterinary Sciences, Faculty of Agronomy, South Campus, University of Chile, Santa Rosa 11735. La Pintana, Santiago, Chile

[3] Escuela de Química y Farmacia, Facultad de Medicina, Universidad Andrés Bello, Sazié 2320, Santiago, Chile

[4] Laboratorio Polyforms. Departamento de Ciencias Biológicas Animales, Facultad de Ciencias Veterinarias y Pecuarias, Universidad de Chile. Santa Rosa 11735, La Pintana, Santiago, Chile

* Correspondence: aneira@uchile.cl (A.N.-C.); sbucarey@uchile.cl (S.A.B.); Tel.: +56-229785674 (A.N.-C.); +56-229785658 (S.A.B.)

Abstract

Sulfated chitosan (ChS) is a chemically modified polysaccharide derived from chitin that mimics heparan sulfate (HS) structures and has emerged as a promising antimicrobial biomaterial. *Piscirickettsia salmonis* (*P. salmonis*), the etiological agent of Salmonid Rickettsial Septicemia (SRS), represents the main driver of antibiotic use in Chilean aquaculture. In this study, the in vitro antibacterial activity of ChS against *P. salmonis* was evaluated. Elemental characterization by SEM-EDS confirmed successful sulfation of the polymer, with a degree of sulfation ranging from 0.92 to 0.95. Antibacterial assays revealed a minimum inhibitory concentration (MIC) of 1500 μg/mL and a minimum bactericidal concentration (MBC ≥1500 μg/mL). LIVE/DEAD™ fluorescence imaging showed the formation of bacterial aggregates with increasing size, frequency, and red fluorescence compared to controls over the exposure to ChS, indicating progressive membrane damage. This was supported by a reduction ($p < 0.05$) in the Green/Red fluorescence ratio of 37–46% between 5h and 96h of exposure, corresponding to alteration of cell membrane. Scanning-electron-microscopy revealed pronounced morphological alterations by ChS, including surface disruption and loss of cellular integrity. This was more severe compared to native chitosan. Also, ChS reduced ($p < 0.05$) biofilm formation (>50% at day 6 and 34.8% at day 8). These results demonstrated that ChS disrupts cell membrane and reduces biofilm-formation in *P. salmonis*, which in consequence affects viability. This is currently the first report of the antibacterial effect of ChS as a HS analogue on *P. salmonis*.

Keywords: sulfated chitosan; *Piscirickettsia salmonis;* antibiofilm activity; antibacterial effect; antimicrobial alternative; heparan sulfate mimetic; bacterial membrane disruption

1. Introduction

Piscirickettsia salmonis is the causative of salmonid rickettsial syndrome (SRS), the bacterial disease with the highest prevalence in the Chilean salmon industry, reaching mortality rates of up to 90% when a event occurs [1–3]. SRS produces annual losses exceeding 600 million dollars, with 8 million dollars spent on antibiotic therapy each year. This promotes the risk of antimicrobial

© 2026 by the author(s). Distributed under a Creative Commons CC BY license.

Preprints.org (www.preprints.org) | NOT PEER-REVIEWED | Posted: 1 April 2026 doi:10.20944/preprints202604.0022.v1

resistance (AMR) and has a negative impact on marine environments. Despite the fact that antibiotic use in Chilean salmon farming has decreased, SRS still accounts for 90% of antimicrobials administered in salmon production [1,3–7]. Its facultative intracellular nature and biofilm formation confer to *P. salmonis* low susceptibility to authorized antibiotics in Chilean aquaculture (florfenicol and oxytetracycline) ([8–10], thereby reducing its exposure to these drugs and promoting chronic infections. The FAO has emphasized the urgent need to reduce antibiotic use and promote innovative alternatives for pathogen control in aquaculture [7,11].

Sulfated chitosan (ChS), is a polysaccharide derived from chitin, with chemical modifications that mimic heparan sulfate (HS), a glycosaminoglycan (GAG) found in hosts that is used by various intracellular pathogens for cell adhesion and invasion [12] has been recently used to bind viruses and bacterium [13–15]. The high negative charge density of ChS [16] enables it to interact with bacterial surfaces, with both ionic and non-ionic attractions to negatively charged bacterial membranes, thereby promoting adhesion [17–23]. This could lead to charge modification, membrane destabilization, and possible inhibition of adhesion or biofilm formation. Previous studies have shown that ChS blocks viral and bacterial adhesion through mechanisms that mimic HS [13–16] while also simultaneously being biocompatible, biodegradable, and of low-toxicity [18,19,21,24].

Our research group has previously developed ChS with controlled chemical substitution. These particles have been patented as antimicrobial biomaterials for use in biomedical and biotechnological applications (US Patent 11,246,839 B2). Compared with native chitosan, these materials exhibit enhanced physicochemical properties and improved biological activity [16].

Based on these properties, we hypothesized that ChS might interact with *P. salmonis* via ionic and non-ionic bonds, thereby acting as a HS analogue and impacting bacterial membrane integrity and the aggregation processes. This study aimed to evaluate the in vitro antibacterial activity of ChS against the P. *salmonis* LF-89 strain, including its effects on bacterial viability, membrane integrity, cellular morphology and biofilm production. Understanding these interactions could inform the development of sustainable, biomaterial-based strategies for controlling SRS in aquaculture using a One Health approach.

2. Results

2.1. Elemental Characterization and Degree of Sulfation of Sulfated Chitosan

Energy-dispersive X-ray spectroscopy (EDS) analysis confirmed the presence of the expected main chemical elements for ChS, namely carbon (C), oxygen (O), nitrogen (N) and sulfur (S) (Figure 1). The elemental composition of the sample analyzed was 43.4% C, 41.7% O, 10.1% S, and 4.8% N. This supports the successful chemical modification of the chitosan backbone. The presence of sulfur, which is absent in pristine native chitosan, confirms the incorporation of sulfate groups into the polymer structure. Based on the S/N ratio obtained from the EDS analysis; the degree of sulfation (DS) was estimated to be DS ≈ 0.92–0.95. This indicates that around 0.92–0.95% of the glucosamine units have been replaced by sulfate groups, producing a polymer with important DS. Further elemental mapping revealed a relatively homogeneous distribution of S atoms within the analyzed area, suggesting uniform chemical modification of the chitosan. The introduction of sulfate groups is expected to increase the polymer's negative charge density, thereby modifying its physicochemical properties and potentially affecting its interaction with bacterial cells. These results also indicate a high DS, suggesting that most of the available amino or hydroxyl groups in the glucosamine units were successfully replaced by sulphate groups.

© 2026 by the author(s). Distributed under a Creative Commons CC BY license.

Preprints.org (www.preprints.org) | NOT PEER-REVIEWED | Posted: 1 April 2026 doi:10.20944/preprints202604.0022.v1

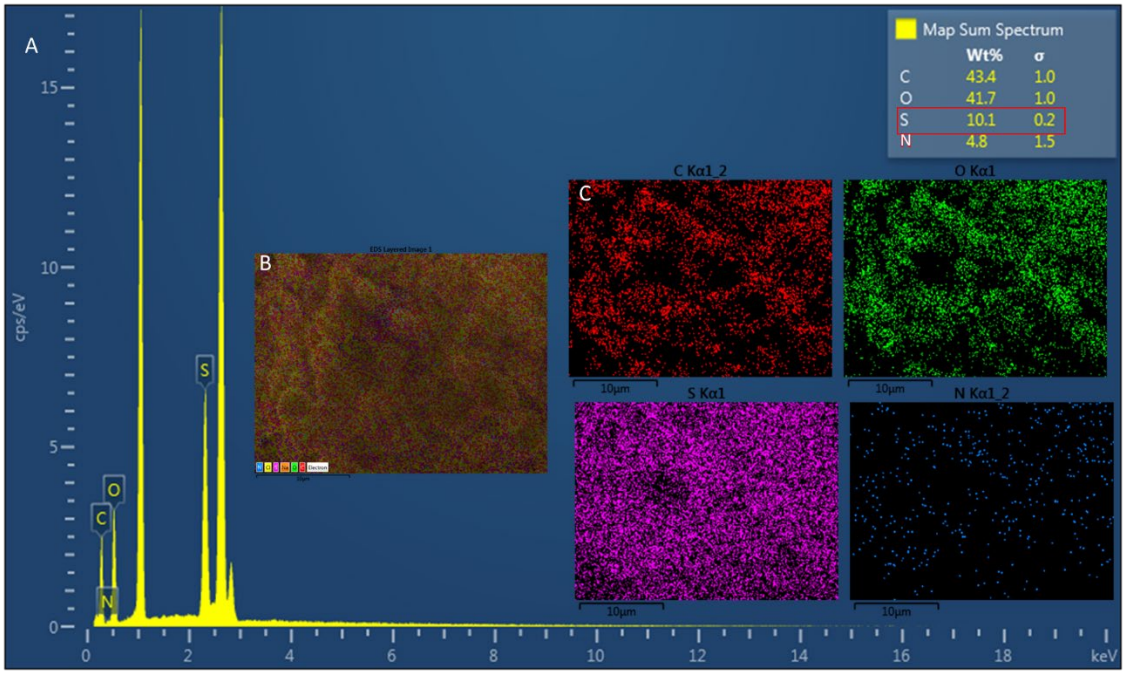

Figure 1. Energy-dispersive X-ray spectroscopy (EDS) analysis and elemental map of sample B. The left panel shows the representative EDS spectrum acquired from the analyzed area, displaying the characteristic peaks of C, O, S, and N. The inset table summarizes the semi-quantitative elemental composition (wt%), indicating that C (43.4 wt%) and O (41.7 wt%) are the predominant elements, followed by S (10.1 wt%) and N (4.8 wt%). The right-hand panels display elemental distribution maps for C (Kα1), O (Kα1), S (Kα1), and N (Kα1). Carbon and sulfur exhibit a relatively homogeneous distribution across the analyzed region, consistent with a carbon-rich sulfur-containing matrix. Oxygen shows a moderate and uniform signal, whereas nitrogen appears at lower intensity and is more sparsely distributed.

2.2. Antibacterial Activity

The antibacterial activity of ChS and ChC against Piscirickettsia salmonis LF-89 was evaluated by determining their minimum inhibitory (MIC) and minimum bactericidal (MBC) concentrations. The results are summarized in Figure 2 and Table 1. ChS exhibited a MIC of 1500 µg/mL, whereas ChC required 3000 µg/mL to inhibit bacterial growth. These results suggest that the sulfation reaction doubled the antibacterial activity of chitosan against *P. salmonis*. In contrast, the antibiotics currently authorized for use in Chilean aquaculture exhibited significantly greater antibacterial potency. Oxytetracycline (OTA) and florfenicol (FF) displayed MIC values of 3.9 µg/mL and 4 µg/mL, respectively. Based on these values, OTA and FF were approximately 385 and 375-fold more potent than ChS respectively.

© 2026 by the author(s). Distributed under a Creative Commons CC BY license.

Preprints.org (www.preprints.org) | NOT PEER-REVIEWED | Posted: 1 April 2026 doi:10.20944/preprints202604.0022.v1

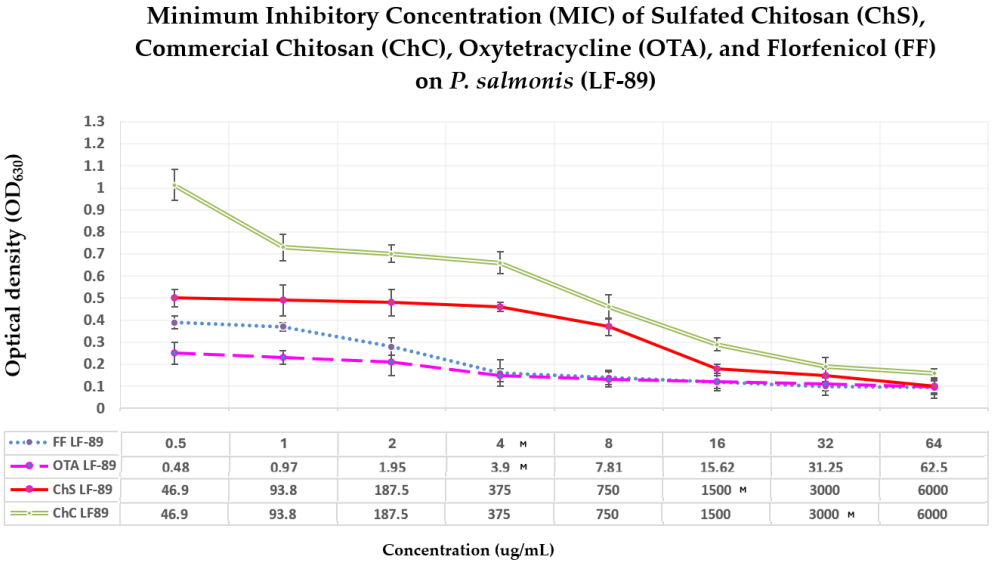

Figure 2. The minimum inhibitory concentration (MIC) of chitosan derivatives and antibiotics against *P. salmonis* LF-89. The figure shows the MIC values obtained for ChS, ChC, OTA, and FF. The letter M indicates the MIC of each active ingredient. Optical density measurements were used to determine bacterial growth inhibition. ChS exhibited a MIC of 1500 μg/mL, whereas ChC required 3000 μg/mL to inhibit bacterial growth. In contrast, OTA and FF showed lower MIC values (3.9 μg/mL and 4 μg/mL, respectively), indicating higher antibacterial potency. The results also demonstrate a concentration-dependent inhibitory effect of chitosan derivatives on *P. salmonis*.

Table 1. Relative potency compared to the MIC of ChS, vs. ChC, OTA and FF against *P. salmonis* strains LF-89.

Treatment	MIC (μg/mL)	MBC (μg/mL)	MBC (μg/mL)
ChS	1500	≥ 1500	Relative potency compared to the MIC of ChS
ChC	3000	≥ 3000	2 times less potent
OTA	3.9	≥ 3.9	~ 385 times more potent
FF	4	≥ 4	~ 375 times more potent

MBC: minimum bactericidal concentration; MIC: minimum inhibitory concentration.

Despite having lower intrinsic potency than conventional antibiotics, ChS exhibited a clear, concentration-dependent inhibitory effect on P. *salmonis* during the 144-hour incubation period. Notably, comparing ChS with native Ch shows that the sulfation reaction substantially enhances the biopolymer's antibacterial activity.

2.2.1. Bacterial Viability and Bacterial Membrane Permeability

Bacterial membrane permeability after exposure to chitosan derivatives was evaluated using LIVE/DEAD fluorescence staining, which measures the ratio between green fluorescence (SYTO9, intact cell membranes) and red fluorescence (propidium iodide, damaged membranes). A higher Green/Red fluorescence ratio indicates a normal cell membrane structure and function, whereas lower values reflect increased membrane permeabilization and contributes to studying the decrease in viability, associated with other studies (such as SEM in bacteria and inoculation in culture media, to demonstrate absence of bacterial growth). During the early exposure phase (10–30 min), no statistically significant differences ($p > 0.05$) were detected between the chitosan treatments and the untreated control (Figure 3). By contrast, ethanol used as a positive control for membrane disruption produced a rapid and significant reduction in bacterial viability within the first 10 min of exposure ($p < 0.05$).

© 2026 by the author(s). Distributed under a Creative Commons CC BY license.

Preprints.org (www.preprints.org) | NOT PEER-REVIEWED | Posted: 1 April 2026 doi:10.20944/preprints202604.0022.v1

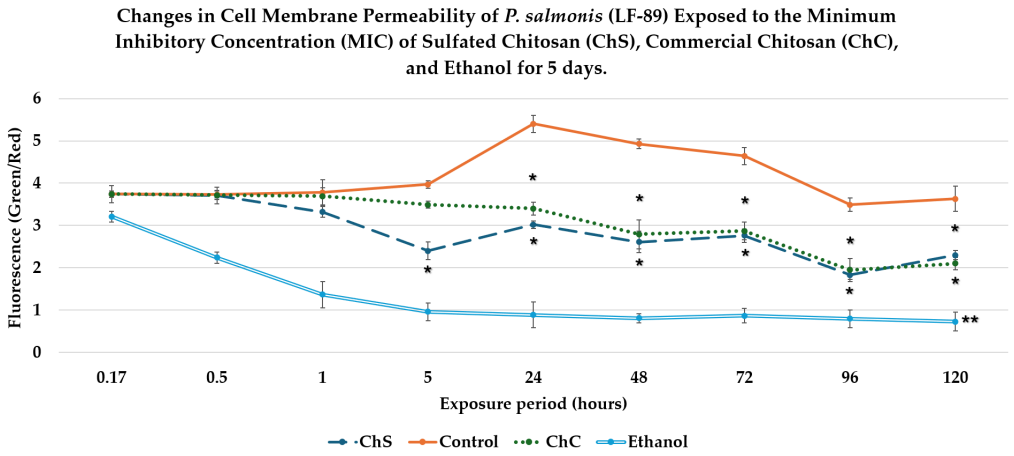

Figure 3. Changes in bacterial membrane permeability of *P. salmonis* are shown following exposure to ChS, ChC and ethanol for a period of 5 days (120 hours of incubation), compared to inoculum control. Cell membrane permeability was assessed using LIVE/DEAD fluorescence staining based on the ratio between green fluorescence (SYTO9, viable cells) and red fluorescence (propidium iodide, membrane-damaged cells). The decrease in the Green/Red ratio indicated greater intracellular propidium iodide (PI) uptake and, therefore, greater alteration of the bacterial cell membrane. Cultures were exposed to MIC of ChS (1500 μg/mL) and ChC (3000 μg/mL). Ethanol (50%) was used as a positive control for membrane disruption. The data represents the mean fluorescence ratio obtained from three independent replicates over a 5-day period. Asterisks indicate statistically significant relative to the untreated control ($p < 0.05$), whereas double asterisks indicate stronger significance ($p < 0.01$) of ethanol after 30 min.

After 1 h of exposure, both biopolymers exhibited a slight decrease in the green/red fluorescence ratio compared to the control, though these differences were not statistically significant. ChS was tested at its MIC of 1500 μg/mL, whereas ChC required a higher concentration of 3000 μg/mL.

Clear treatment-dependent differences became evident during the intermediate exposure period (5–48 h). At 5 h, the control inoculum maintained stable membrane permeability values, whereas ChS significantly reduced the Green/Red fluorescence ratio compared with both the control and the ChC treatment ($p < 0.05$). Between 24 and 48 h, both chitosan derivatives induced a significant reduction in Green/Red fluorescence ratio relative to the control ($p < 0.05$).

Despite the difference in MIC values, no statistically significant differences were detected between ChS and ChC during this period, suggesting comparable effects once the polymers reached their effective concentrations. During prolonged exposure (72–120 h), the untreated control maintained consistently high values of fluorescence ratio, indicating a stable membrane permeability in the absence of treatment. By contrast, both chitosan derivatives were found to produce a sustained reduction in Green/Red fluorescence ratio ($p < 0.05$), which confirms the presence of a time-dependent effect. Also, the *P. salmonis* cells that were subsequently cultured in Austral-SRS medium for 14 days to evaluate bacterial recovery showed no detectable growth after 120 hours of exposure to the treatments, indicating a time-dependent lethality effect.

Overall, the Green/Red fluorescence ratio assay indicates that exposure to chitosan polymers results in a progressive increase in bacterial membrane permeability of *P. salmonis*. Notably, ChS produced effects comparable to those of ChC when applied at half the concentration (1500 μg/mL versus 3000 μg/mL), supporting the idea that polymer sulfation enhances antibacterial efficiency. Ethanol acted as an effective positive control, inducing rapid and sustained increase in the bacterial membrane alteration.

© 2026 by the author(s). Distributed under a Creative Commons CC BY license.

Preprints.org (www.preprints.org) | NOT PEER-REVIEWED | Posted: 1 April 2026 doi:10.20944/preprints202604.0022.v1

2.3. Fluorescence Microscopy Analysis

Fluorescence microscopy with LIVE/DEAD staining was used to assess the integrity of the membrane in P. salmonis after exposure to chitosan derivatives. This staining method uses two fluorophores: SYTO9, which penetrates all cells and emits green fluorescence, and (propidium iodide (PI)), which only penetrates cells with compromised membranes and emits red fluorescence. When both dyes are present intracellularly, PI displaces SYTO9, resulting in predominant red fluorescence, which indicates membrane damage. In the untreated control group, bacterial cells displayed predominantly green fluorescence with minimal red signal (Figure 4A). The cells were mostly isolated and distributed homogeneously, with no evident bacterial micro aggregates, indicating preserved membrane integrity during the experiment.

Exposure to 50% ethanol, which was used as a positive control for membrane disruption, produced a rapid increase in red fluorescence, accompanied by a reduction in green fluorescence. This result is consistent with the known mechanism of ethanol in Gram-negative bacteria, which involves disruption of the bacterial membrane. In cultures exposed to commercial chitosan (ChC), both green and red fluorescence signals were detected (Figure 4B–C). Small bacterial aggregates were observed after 5 h of exposure, with green fluorescence predominating and limited red fluorescence. After prolonged exposure (96 h), aggregates became more frequent but did not show substantial increases in size. Red fluorescence remained relatively diffuse and less intense within these aggregates, suggesting partial membrane permeabilization.

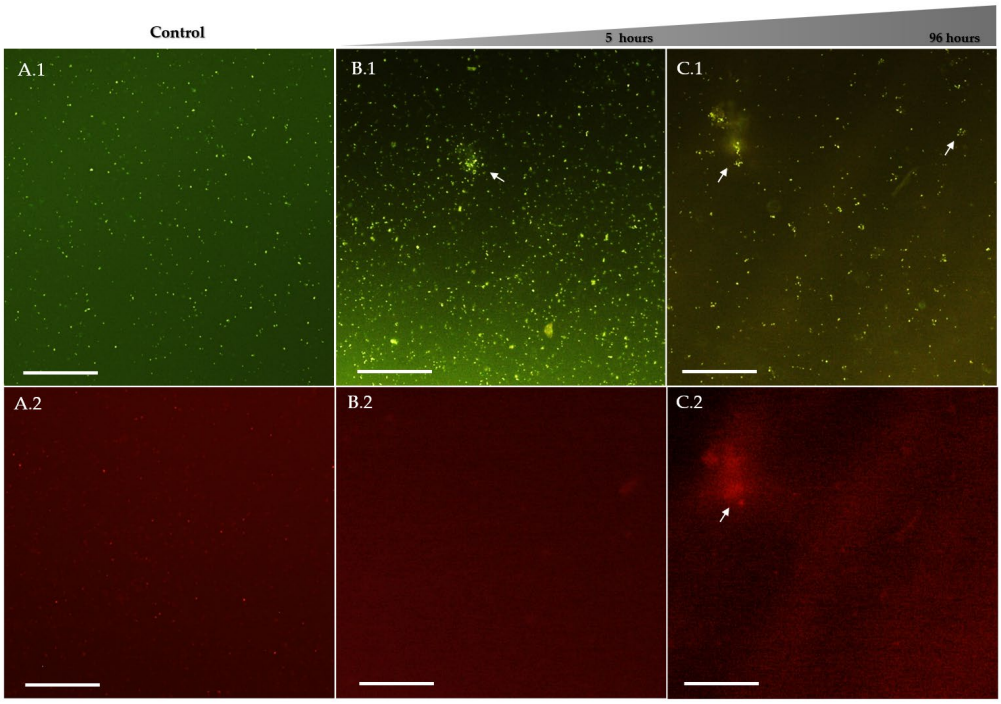

Figure 4. Fluorescence microscopy of *P. salmonis* (LF-89) stained with LIVE/DEAD fluorescent dyes. Bacterial cultures were stained with SYTO9 (green fluorescence, intact cell membranes) and PI (red fluorescence, membrane-damaged cells). Images A.1 and A.2 correspond to the untreated inoculum control, showing predominantly green fluorescence with minimal red signal, indicating preserved membrane integrity and mostly isolated bacterial cells without evident microaggregation. Images B.1 and B.2 show bacteria after 5 h exposure to ChC at its MIC (3000 μg/mL), where small bacterial aggregates with predominant green fluorescence and limited red fluorescence are observed. Images C.1 and C.2 correspond to 96 h exposure to ChC, showing more frequent bacterial aggregates compared with the earlier exposure period. In these aggregates, green fluorescence remains predominant while red fluorescence appears diffuse and less intense, suggesting partial membrane permeabilization. Magnification: 10× (Scale bar = 100 μm).

© 2026 by the author(s). Distributed under a Creative Commons CC BY license.

Preprints.org (www.preprints.org) | NOT PEER-REVIEWED | Posted: 1 April 2026 doi:10.20944/preprints202604.0022.v1

In contrast, cultures exposed to ChS exhibited more pronounced alterations in fluorescence patterns (Figure 5). After 5 h of exposure, bacterial micro aggregates were already visible, with predominant green fluorescence and limited red signal. However, between 24 and 48 h, a clear increase in red fluorescence was observed within the aggregates, indicating progressive membrane permeabilization. During prolonged exposure (72–120 h), aggregates became larger and more frequent, and the red fluorescence became comparable to or greater than the green fluorescence. This suggests extensive membrane damage and increased PI penetration.

These qualitative observations are consistent with the quantitative membrane cell permeability data obtained through fluorescence measurements. These measurements showed a progressive decrease in the Green/Red fluorescence ratio following exposure to ChS.

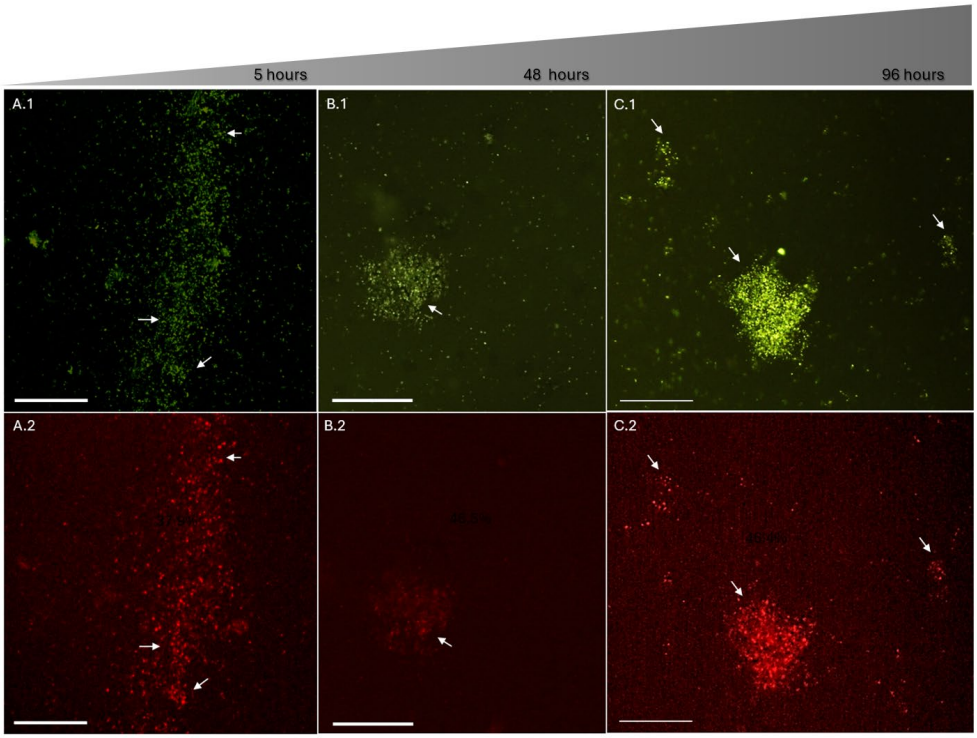

Figure 5. Fluorescence microscopy of *P. salmonis* (LF-89) after exposure to sulfated chitosan (ChS). *P. salmonis* stained with LIVE/DEAD fluorescent dyes. Bacterial cultures stained with SYTO9 (green fluorescence, intact cell membranes) and PI (red fluorescence, membrane-damaged cells). Images A.1 and A.2 show bacteria after 5 h exposure to ChS at its MIC (1500 µg/mL), where green fluorescence predominates and small bacterial microaggregates are visible (arrows). Images B.1 and B.2 correspond to 48 h exposure, showing increased red fluorescence and the formation of larger and more compact aggregates, with mixed green and red fluorescence within the same field. Images C.1 and C.2 correspond to 96 h exposure, where aggregates appear larger and more frequent, and red fluorescence becomes comparable to or greater than green fluorescence, indicating progressive membrane damage and increased permeability to PI. Magnification: 10× (Scale bar = 100 µm).

These observations are supported by quantitative fluorescence analysis (Figure 6), which shows a significant decrease in the Green/Red fluorescence ratio after exposure to ChS. As shown in Figure 6, exposure to ChS reduced Green/Red ratio by 37.9%, 46.5%, and 46.4% at 5, 48, and 96 h, respectively, compared with the untreated control.

© 2026 by the author(s). Distributed under a Creative Commons CC BY license.

Preprints.org (www.preprints.org) | NOT PEER-REVIEWED | Posted: 1 April 2026 doi:10.20944/preprints202604.0022.v1

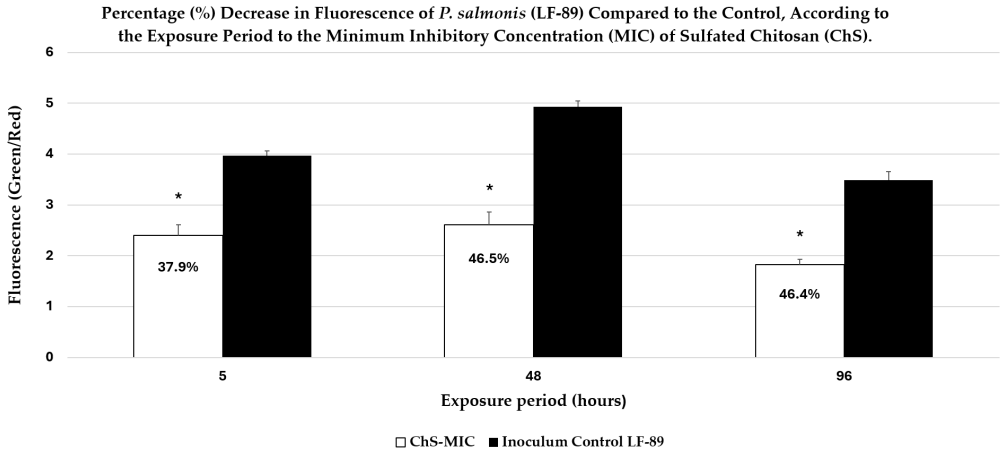

Figure 6. Decrease in Green/Red ratio of *P. salmonis* after exposure to ChS-MIC. Bacterial membrane permeability was assessed using LIVE/DEAD staining and expressed as the Green/Red fluorescence ratio. Cultures were exposed to ChS at its MIC (1500 µg/mL) and data are shown of 5, 48, and 96 h. ChS reduced ($p < 0.05$) the Green/Red ratio compared with the untreated control *($p < 0.05$). The decrease in the Green/Red ratio indicated greater intracellular PI uptake and, therefore, greater alteration of the bacterial cell membrane.

2.4. Scanning Electron Microscopy (SEM) Analysis

Scanning electron microscopy (SEM) was used to examine the morphological alterations in *P. salmonis* cultures that were exposed to the MIC of ChS and ChC for 24 h (Figure 7). Control cultures of *P. salmonis* without chitosan polymer derivatives exposure displayed spherical to coccoid bacterial cells with relatively smooth surfaces and well-defined cellular boundaries (Figure 7A–A.1). The bacteria were frequently observed as isolated cells and occasionally forming small microclusters. The cell morphology appeared intact, with no visible surface depressions or structural alterations. Cultures exposed to the MIC of ChC showed moderate morphological changes compared to the control (Figure 7B). Although most bacterial cells retained their spherical morphology, surface roughness and slight deformation of the coccoid shape were evident. The cells frequently appeared clustered and partially embedded within a matrix-like structure; however, the cell boundaries remained distinguishable in most areas.

In contrast, cultures exposed to the ChS MIC exhibited significantly more pronounced morphological alterations (Figure 7C–D). Large irregular aggregates composed of densely packed bacterial cells were observed, accompanied by extensive cell coalescence and loss of clear intercellular boundaries. At higher magnification, cells showed surface depressions, reduced intracellular volume, and severe distortion of the outer cell envelope. The formation of compact aggregates and the loss of normal coccoid morphology suggest strong interactions between bacterial cells and the sulfated chitosan polymer. These structural alterations were more extensive and frequent than those observed in cultures treated with ChC. Overall, SEM analysis indicates that exposure to ChS induces substantial structural damage in *P. salmonis*, consistent with the membrane disruption observed using fluorescence microscopy and with the reduction in Green/Red ratio (Increased intracellular PI uptake) by fluorescence assays. Also, the *P. salmonis* cells that were subsequently cultured in Austral-SRS medium to evaluate bacterial recovery showed no detectable growth after 120 hours of incubation with the treatments. This finding, in the case of ChS, complements the results of the Green/Red ratio studies and SEM images, and is consistent with a possible mechanism of action of ChS based on disruption of the cell membrane, which could irreversibly compromise bacterial viability.

© 2026 by the author(s). Distributed under a Creative Commons CC BY license.

Preprints.org (www.preprints.org) | NOT PEER-REVIEWED | Posted: 1 April 2026 doi:10.20944/preprints202604.0022.v1

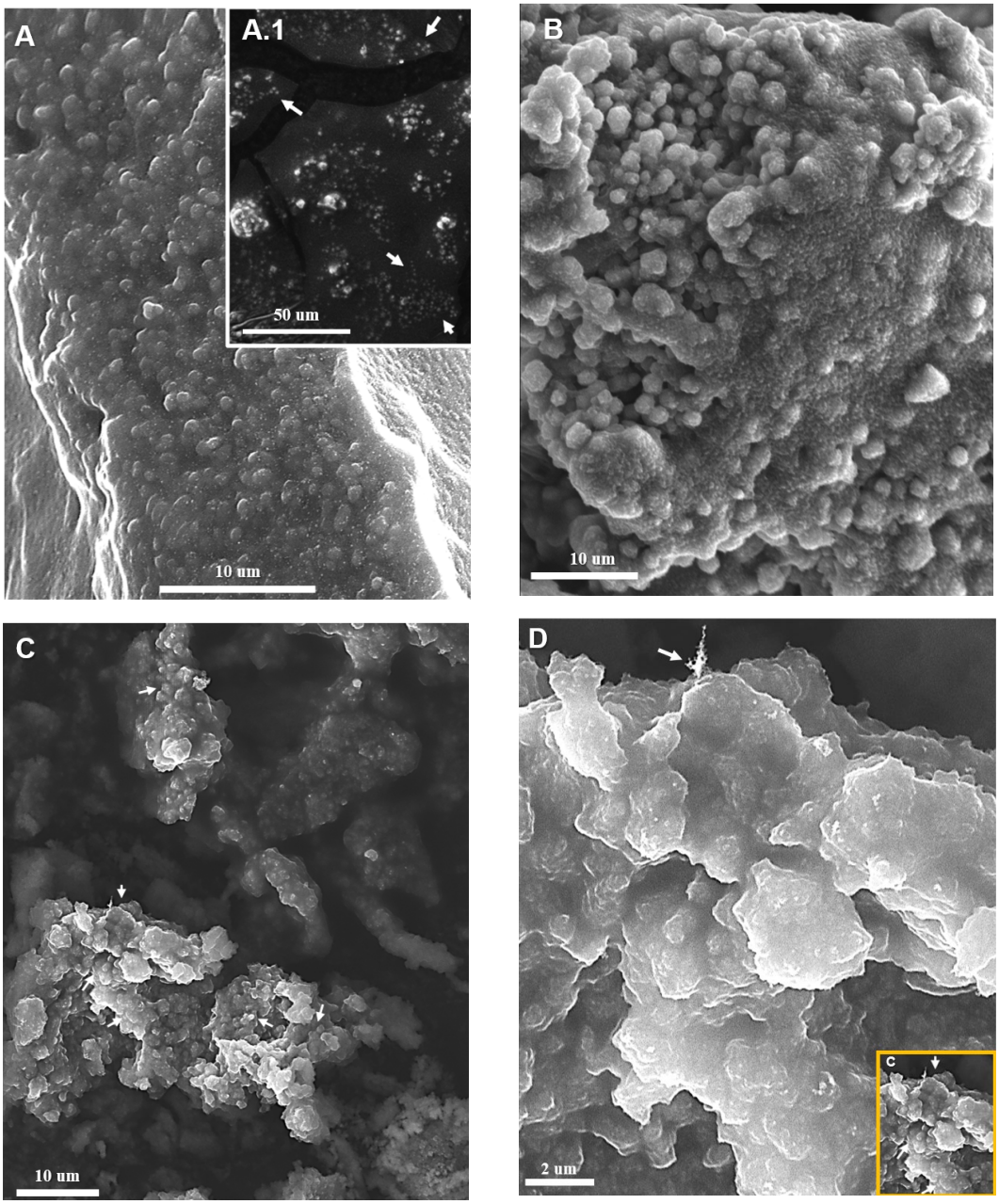

Figure 7. Scanning electron microscopy of *P. salmonis* was exposed to chitosan derivatives. Morphological comparison of *P. salmonis* (LF-89) cultures after 24 h exposure to the minimum inhibitory concentrations of commercial chitosan (ChC) and sulfated chitosan (ChS). (A) Micrograph (x2500): Untreated control showing spherical and coccoid bacteria with smooth surfaces, well-defined cell boundaries and intercellular demarcation is distinguishable (arrow). (A.1) Micrograph (x300): Image of the inoculum control at lower magnification showing more dispersed bacteria (arrows) and with little bacterial aggregate formation. (B) Micrograph (x1900): Cultures exposed to ChC (3000 µg/mL), showing moderate surface roughness, bacterial aggregation and reduced preservation of coccoid shape. (C) Micrograph (x1500): Cultures exposed to ChS (1500 µg/mL), showing large compact aggregates, loss of cellular contours (arrows) and intercellular demarcation is not distinguishable. (D) Magnification of micrograph C (x6500): Surface irregularities, and severe distortion of the bacterial envelope (arrow), without distinction of intercellular boundaries.

3. Evaluation of Biofilm Production

Biofilm formation was evaluated during the 4 days of incubation. The untreated bacterial control exhibited a mean OD of 0.433 ± 0.044 indicating initial biofilm establishment under the experimental conditions (Figure 8). According to the Stepanović classification method, the strain was categorized

© 2026 by the author(s). Distributed under a Creative Commons CC BY license.

Preprints.org (www.preprints.org) | NOT PEER-REVIEWED | Posted: 1 April 2026 doi:10.20944/preprints202604.0022.v1

as a weak biofilm producer. This suggests that, at this early stage, biofilm formation is not yet fully developed. The antibiotic control exhibited markedly lower biofilm (0.177 ± 0.019), corresponding to a 59.1% reduction ($p < 0.05$) relative to the untreated control. Treatment with ChS at 750 µg/mL resulted in an increase (0.604 ± 0.053), suggesting a slight stimulation of biofilm formation relative to the control. In contrast, ChS at 1500 µg/mL yielded an OD of 0.421 ± 0.067 representing a minimal reduction of 2.8% ($p > 0.05$), indicating a negligible inhibitory effect at this time point. Conversely, the OTA-treated group (the antibiotic control) showed a significant reduction in biofilm formation compared to all other groups ($p < 0.001$).

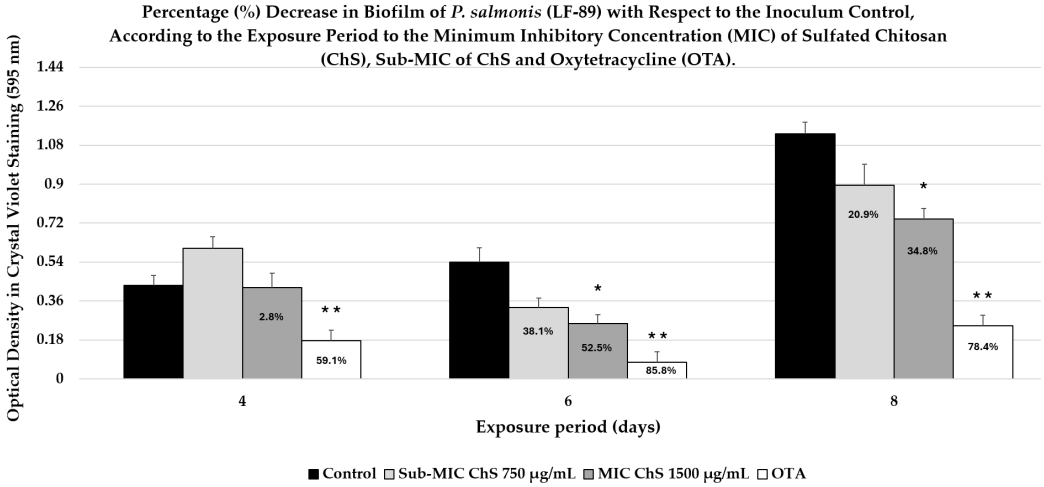

Figure 8. Percentage reduction of biofilm in *P. salmonis* cultures exposed to ChS MIC (1500 µg/mL), Sub-MIC (750 µg/mL), and OTA (5 µg/mL) as a positive control, compared to the untreated control, according to the number of days of experimental incubation. A reduction ($p < 0.05$) in biofilm was observed when the bacteria were exposed to ChS MIC on days 6 and 8 of incubation compared to the inoculum control. The Crystal Violet staining method allowed for the identification of statistically significant differences (* $p < 0.05$ and ** $p < 0.01$) between treatments, based on the optical density (OD corrected) reading. .

During 6 days of incubation period, it is important to note that, according to Stepanović's classification method, the biofilm production by the strain at 6 days was classified as weak. However, the amount of biofilm quantified after 6 days (OD = 0.539 ± 0.068) increased compared to 4 days of incubation (see Figure 8). In this context, the untreated bacterial control exhibited the greatest biofilm biomass compared to the other groups. Conversely, treatment with ChS resulted in a dose-dependent reduction in biofilm formation. Specifically, ChS at concentration of 750 µg/mL reduced biofilm formation by 38.6%. This decrease was not significant ($p > 0.05$) compared to the control; however, increasing the concentration to 1500 µg/mL resulted in a 52.5% reduction ($p < 0.05$), indicating improved antibiofilm activity from exposure to the MIC of ChS. The most pronounced effect was produced by the positive control (OTA, 5 µg/mL), with an 85.9% reduction in bio-film biomass ($p < 0.001$), which confirms both the sensitivity of the assay and the validity of the experimental design.

After 8 days of incubation, the bacterial control showed an average optical density (OD) of 1.133 ± 0.053, indicating an increase in adhered biofilm biomass compared to previous experimental times (Figure 8). According to Stepanović's classification, the strain was categorized as a moderate biofilm producer, which is consistent with the high OD values observed in the control group during this experimental period. The evaluation of the treatments revealed a differential reduction in biofilm formation. ChS at 750 µg/mL showed an OD of 0.896 ± 0.096 corresponding to a 20.9% decrease compared to the control. However, this effect was not statistically significant ($p > 0.05$), suggesting that, although there is an inhibitory trend, the experimental variability in this group may have prevented the detection of statistical significance, but a biological decrease was evident.

© 2026 by the author(s). Distributed under a Creative Commons CC BY license.

Preprints.org (www.preprints.org) | NOT PEER-REVIEWED | Posted: 1 April 2026 doi:10.20944/preprints202604.0022.v1

In contrast, the MIC of ChS (1500 µg/mL) showed an OD = 0.739 ± 0.049 with a 34.8% reduction, which was statistically significant ($p < 0.05$). This finding demonstrates a dose-dependent effect, indicating that increasing the ChS concentration allows it to exceed the threshold necessary to significantly interfere with biofilm maturation or production. For its part. The antibiotic control treatment exhibited the greatest inhibitory efficacy in this experimental period, with an OD = 0.245 ± 0.04, equivalent to a 78.4% decrease ($p < 0.01$) compared to the control. This result validates the model using positive control, which remained constant throughout the three experimental periods, demonstrating superior inhibitory capacity regardless of the biofilm's maturation stage.

4. Discussion

The MIC results indicated a concentration-dependent effect of ChS on *P. salmonis* in vitro. While the licensed antibiotics for use in aquaculture (FF and OTA) have lower MIC than chitosans (ChS and ChC). Unmodified chitosan generally exert their action through non-specific mechanisms on the cell membrane or other bacterial structures [25,26]. ChC usually require a higher MIC than licensed antibiotics and chemical modifications are necessary to improve its potency, efficacy, or bioavailability according to previous reports for polymer-based antimicrobial agents [27–29]. ChS showed a 50% reduction in MIC compared to ChC, suggesting that the chemical surface modification increases its interaction with the bacterial surface. These results indicate that, although chitosan required higher concentrations to inhibit bacterial growth, its progressive antibacterial effect, low potential for resistance generation, low toxicity, and minimal environmental impact [18,19,24,26,30] position it as a complementary or alternative antimicrobial candidate in *P. salmonis* control strategies.

The combination of results from membrane integrity analysis (qualitative and quantitative) by fluorescence microscopy and morpho-structural findings by SEM analysis demonstrated distinct antibacterial behaviors between ChS and ChC. The ChC induced less membrane disturbance and limited structural deformation, suggesting surface-related interactions that compromise membrane permeability without inducing extensive structural collapse.

In contrast, ChS produced progressive membrane destabilization, accompanied by greater and more evident structural damage. The relationship between increased PI incorporation and ultrastructural deformation supports an antibacterial mechanism driven by sustained membrane disruption. The time-dependent decrease in the Green/Red ratio after 120 h of exposure indicated that the presence of sulphate groups increased its antimicrobial potency of chitosan by promoting progressive membrane permeabilization. This was associated with irreversible ultrastructural changes to the bacterial outer surface (Figure 7).

Additionally, it is necessary to distinguish between the formation of bacterial aggregates, which increase in size and frequency with exposure time to ChS. Similar aggregation phenomena have been reported for other modified polysaccharides and are thought to be due to polymer-mediated cross-linking of bacterial cells [27,31]. Similar mechanisms have been proposed for other antimicrobial polymers which are associated with membrane disruption and leakage of intracellular contents [32].

It is important to note that the reports on *P. salmonis* exposure to modified or unmodified chitosan are absent or scarce. However, regarding this aspect, some researchers [33] discuss the findings described by other authors [34–36], that unmodified, high molecular weight, polycationic chitosans can form a dense polymer film on the cell surface. This blocks nutrient exchange by coating the porins of the outer membrane of Gram-negative bacteria, causing bacterial death. According to these authors, this pattern was identified by observing detected through the thickening of cell walls, indicating the deposition of chitosan on the cell surface [36]. It was also reported here that the flocculation effect can be detected using SEM, which shows vesicular structures in the outer membrane of *E. coli* and *S. typhimurium* treated with chitosan [34].

Other studies [37] described the antibacterial activity of ferulic-acid-grafted chitosan derivatives against *L. monocytogenes*, *P. aeruginosa*, and *S. aureus*. This modified chitosan retained the cationic character of the polymer backbone, allowing strong interactions with bacterial cell surfaces, according to the authors. Fluorescence staining using PI demonstrated increased membrane

© 2026 by the author(s). Distributed under a Creative Commons CC BY license.

Preprints.org (www.preprints.org) | NOT PEER-REVIEWED | Posted: 1 April 2026 doi:10.20944/preprints202604.0022.v1

permeability and described that the cells were found in aggregates (size: 10–500 μm), while SEM observations exhibited profound changes in the cell morphology and cells largely clustered together to appear in aggregates with gross increase in cell size when compared to their corresponding untreated controls. The authors proposed that adsorption of cationic chitosan derivatives onto bacterial membranes could alter cell–cell interactions and potentially contribute to localized cellular aggregation during the antimicrobial process.

In contrast, other reports on the antibacterial activity of films with modified polycationic chitosans (graphene oxide among other derivatives) were evaluated in *Campylobacter jejuni* and *Listeria monocytogenes*. The authors reported similar approaches combining live/dead fluorescence staining with SEM, since increased PI uptake indicates membrane permeabilization. SEM images revealed cell wall disruption and leakage of intracellular components, which is consistent with the classic mechanism of electrostatic interaction between polycationic chitosan and bacterial surfaces. However, they did not describe the phenomenon of bacterial aggregation [38].

Other authors exposed *S. aureus*, *P. aeruginosa* and *E. coli* to silver (Ag) nanoparticles combined with chitosan and demonstrated bacterial aggregate formation (by confocal laser scanning microscopy) in all three species with these polycationic nanocomposites at the highest tested chitosan concentrations. Aggregates were more evident and frequent in *E. coli* than in the other species, suggesting that this cell aggregation may contribute to the increased bactericidal activity observed in *E. coli*. However, in *S. aureus*, aggregate formation was also observed at sublethal concentrations of the nanocomposite [31].

In the current work, the formation of large aggregates observed in the SEM and fluorescence images suggests that ChS may promote the formation of polymer-bacteria complexes and was possibly associated with antibacterial activity. However, the formation of cell aggregates in bacteria exposed to chitosan, with or without modifications, is a variable phenomenon whose complexity still requires further investigation. Although some of the authors cited previously associate bacterial aggregation with the antibacterial effects of exposure to these polymers, Laanoja et al. [31] argue that greater importance should be given to studying bacterial cell aggregates. These reports describe how interactions between bacteria and harmful nanoparticles could induce disruption of the cell membrane, causing leakage of intracellular content, and modulation of cell surface properties. This could trigger the production of extracellular polymeric substances and promote bacterial aggregation as a defensive response [39].

In this regard, previous studies [40] have demonstrated that *P. salmonis* can form structured cellular aggregates under nutrient-limited conditions (48 h), in contrast to bacteria cultured in nutrient-rich conditions. Also, enzymatic treatment with cellulose led to marked disaggregation of these structures, suggesting that they were stabilized by an extracellular polymeric substance (EPS) matrix, a characteristic feature of biofilms. SEM further revealed that these aggregates corresponded to dense, three-dimensional structures in which bacterial cells were embedded within a rigid extracellular matrix. The authors proposed that this EPS-mediated aggregation acts as a protective strategy, facilitating environmental persistence and host colonization.

In contrast, the microaggregates observed following exposure to both ChS and ChC do not display features consistent with mature EPS-embedded biofilms. Instead, SEM analysis revealed irregular clustering of bacterial cells (with morphological changes on the surface) lacking a continuous extracellular matrix, suggesting a distinct aggregation mechanism (Figure 7). Given that these experiments were conducted in nutrient-rich SRS medium supplemented (fetal bovine serum, L-cysteine and iron), conditions that do not typically induce EPS-driven aggregation, after 48 h of incubation and shaking. The observed clustering is more likely associated with physicochemical interactions induced by the polymers rather than a canonical biofilm developmental process. Notably, aggregation was more pronounced in the presence of ChS, indicating that polymer-induced cell clustering may occur independently of classical electrostatic interactions described for chitosan without modification. This suggests that alternative mechanisms, such as polymer bridging, surface

© 2026 by the author(s). Distributed under a Creative Commons CC BY license.

Preprints.org (www.preprints.org) | NOT PEER-REVIEWED | Posted: 1 April 2026 doi:10.20944/preprints202604.0022.v1

adsorption, or modulation of intercellular forces, may contribute to bacterial aggregation under these conditions.

This work provides evidence of bacterial aggregates occurring with a sulphur-modified chitosan, which has a net negative charge. Therefore, the formation of bacteria-ChS complexes between this polymer and *P. salmonis* cannot be explained exclusively by electrostatic or polar attractions, as is the case with polycationic chitosans. However, bacterial aggregation could occur differently with modified chitosans, depending on the derivative type or functionalization [21,25,26].

This previously described pattern may differ for ChS due to its structural biomimicry with HS, its net negative charge resulting from sulphur functionalization and its low molecular weight. The successful incorporation of sulphate groups into the chitosan structure was confirmed by established deacetylation levels [16] and elemental characterization, achieving a degree of sulfation of 0.92–0.95 in the present study. This level of substitution is consistent with previously reported sulfated chitosan derivatives exhibiting biological activity while maintaining the structural stability of the polymer matrix [18].

Previous reports, using sulfated chitosan (5.6041%, 6.0045%, and 6.8051%), describe moderate antibacterial activity with a broad spectrum against *E. coli* and *S. aureus*. It was observed that the antimicrobial activity against both types of bacteria increased proportionally to the degree of sulfation [41]. According to the authors, trials involving an 86% degree of sulfation increased the negative charge of the native polymer and the antibacterial activity was more effective against *E. coli* than *S. aureus*, suggesting that this derivative showed greater antibacterial activity against Gram-negative bacteria [42].

In this sense, the increased antibacterial activity of sulfated modified chitosans [43] supports the results of the present research. Combined with other reported variables, such as polymer concentration and size, ambient pH, Gram-negative bacterial species [25,26,44,45], and, probably, the bacterial exposure period to the biopolymer, this suggests a different pattern of antibacterial activity to that of native or polycationic chitosans.

According to some authors, one explanation for this property of sulfur-modified polymers as a biomimetic of HS may be due to the existence of residual amino groups in the structure of these polymers, which might give it polyampholytic characteristics present in some sulfated glycosaminoglycans (GAGs), such as HS. This allows them to interact with a wide variety of GAG-binding proteins in the extracellular matrix and mediate various functions, such as adhesion [46], antimicrobial activity [42,47], and effects of intermolecular bonding, protein aggregation, or coagulation [48–50]. In this regard, some authors have described how chitosan derivatives retain some of these biological properties and have demonstrated antibacterial properties [18,23,51,52].

These properties are fundamental, as they suggest that the net negative charge of ChS, like the polyanionic structure of GAGs such as HS [23,47], likely interacts with Gram-negative bacteria without significant restrictions [53–56], such as *P. salmonis*. In this sense, this could facilitate, through previously described mechanisms of ionic and non-ionic interactions [18,23], the binding or adhesion between ChS and *P. salmonis*.

Other authors have reported that the mechanical, chemical, or biological characteristics of chitosans, such as aggregation, molecular agglutination, blood coagulation, or contaminant binding [57–60], are modified or improved depending on their conjugations with other molecules [61–63]. Therefore, the properties of sulfur-containing chitosans mimicking HS, such as bacterial adhesion, protein aggregation, coagulation, or the formation of intermolecular complexes with enzymes/proteins [18,19,21,23,26,47,64–66], may also likely contribute to the alteration of the bacterial membrane by modifying its permeability, given that *P. salmonis* shares conserved structures with Gram-negative bacteria, such as the presence of an outer membrane with lipoproteins, polysaccharides and porins, which likely interacted with ChS as a HS biomimetic [16], producing a comparable effect of protein aggregation, agglutination, or coagulation, through the possible formation of supramolecular complexes between ChS and molecules on the bacterial surface, causing subsequent disruption of membrane integrity.

© 2026 by the author(s). Distributed under a Creative Commons CC BY license.

Preprints.org (www.preprints.org) | NOT PEER-REVIEWED | Posted: 1 April 2026 doi:10.20944/preprints202604.0022.v1

In this context, chemical modification of chitosan is proposed as a strategy to enhance its biological activity and expand its range of applications. Sulfation introduces negatively charged sulfate groups into the polymer backbone, altering its electrostatic properties and enabling interactions that resemble those of GAGs such as HS [18,19,23,26,47,64,65]. Sulfated polysaccharides have been extensively investigated due to their antiviral, antibacterial, and anti-adhesion properties, which are often attributed to their ability to interfere with host–pathogen interactions [19,47], an ability also reported by our research group [13–16].

The results of this study provide information on the antibacterial activity of sulfur-modified chitosans, distinguishing their effect or affinity for the outer membrane of *P. salmonis*. However, the interactions between the external surface of bacteria and the modified polymers remain a complex phenomenon requiring further investigation, especially since the bacterial surface is not a static environment, which could allow for adhesion or intermolecular interactions depending on the environment.

It is worth noting that in intracellular Gram-negative bacteria such as *P. salmonis*, LPS exhibits differences compared to other Gram-negative bacteria, possibly due to its lower surface exposure or structural differences in the core or the O-antigen oligosaccharide, which distinguishes it from other Gram-negative bacteria [67]. Its interactions with sulfated or non-sulfated chitosans may be different or more complex. That is why it is necessary to delve deeper into studies on the possible ionic and non-ionic interactions between the cell membrane of *P. salmonis* and the negatively charged sulfated polymers.

In this context, the likely interactions between ChS and the outer membrane of *P. salmonis* could also interfere with the surface structures that allow adhesion in this bacterium, such as outer membrane vesicles (OMVs) that facilitate the secretion of virulence factors and participate in interbacterial communication and biofilm formation [68–70]. In this regard, type IV pili are present, as well as OmpA-like proteins, which are associated with membrane stability and possible adhesion functions, and autotransporters (TAAs) involved in adhesion processes and possibly biofilm formation [71–73].

Biofilm formation in *P. salmonis* has been experimentally associated with the production of an extracellular polymeric substance (EPS) matrix of predominantly polysaccharide nature [40]. At the molecular level, genomic and functional analyses further support the existence of biosynthetic pathways for surface-associated polysaccharides, including both lipopolysaccharide (LPS) and EPS, indicating that *P. salmonis* possesses the machinery required for production and exporting these polymers. Importantly, EPS in Gram-negative bacteria can remain associated with the outer membrane as a capsule or be released into the extracellular environment, where it contributes directly to biofilm matrix formation [67] . This suggests that in *P. salmonis*, the cell envelope and its polysaccharide components are functionally linked to biofilm development, not only by providing structural elements at the cell surface but also by supplying extracellular polymers that mediate cell aggregation, surface attachment, and matrix stability.

The previous results show that ChS has a concentration-dependent anti-biofilm activity. This effect is significant between 6 and 8 days of exposure, but not in the early (4 days) exposure periods (Figure 8). This effect is possibly due to the interaction of ChS with the previously mentioned structures in the outer membrane of *P. salmonis* that contribute to biofilm formation [40,67–70,73]. Therefore, this anti-biofilm activity is likely associated with the results of this study regarding altered membrane permeability (Figures 3 and 5) and structural modifications of the bacterial envelope (Figure 7). These changes may have contributed to the disorganization of EPS, weakening or modifying the biofilm matrix with ChS through ionic and non-ionic interactions.

Currently, no experimental evaluations have been reported on the effect of pure or modified chitosans on *P. salmonis* biofilm production. However, several important mechanisms of chitosan activity on bacterial biofilms have been distinguished in Gram-negative bacterial models (*E. coli* and *P. aeruginosa*), such as: Interference with bacterial communication strategies (quorum sensing), electrostatic attraction and degradation of the EPS matrix, advanced penetration facilitated by

© 2026 by the author(s). Distributed under a Creative Commons CC BY license.

Preprints.org (www.preprints.org) | NOT PEER-REVIEWED | Posted: 1 April 2026 doi:10.20944/preprints202604.0022.v1

conjugation with specific ligands improving efficacy, even against mature biofilms, in addition to membrane permeabilization and direct antibacterial effects, according to the polycationic nature of chitosans [33,74–77].

Additionally, assays with chitosan modified with sulfur, but retaining its positive charge, demonstrated a dose-dependent reduction in biofilm formation in *P. aeruginosa* ranging from 24.5% to 75% [37]. Other reports used chitosans modified with sulfur, which had a net negative charge, and describe the following: Biofilm inhibition with chitosan nanoparticles loaded with silver sulfadiazine in microbes isolated from wounds [78], significant antibiofilm activity with sulfonated low molecular weight chitosan against *E. coli* and *S. aureus* [79], inhibition of adhesion and biofilm formation with standardized sulfonated biomedical chitosan [80], as well as induction of bacterial death and consequent reduction in biofilm [81], both assays on *P. aeruginosa*.

Although these previous reports did not investigate *P. salmonis*, they indicate that sulfur modifications to native chitosans to change their net charge to negative can decrease or alter biofilm formation in bacteria. This supports the anti-biofilm results in this study, where negatively charged chitosan significantly decreased biofilm formation in *P. salmonis* (Figure 8), ranging from 34.8% to 52%.

Regarding these results, it is worth mentioning that biofilm formation in this bacterium is a complex phenomenon and a virulence factor, and that most research has been conducted in vitro. *P. salmonis* can form biofilms, depending on stressful conditions or environmental challenges, on biotic and abiotic surfaces, allowing it to persist in the marine environment and in aquaculture facilities. This contributes to its transmission and antimicrobial resistance through adaptive gene regulation, ensuring its survival in the host [40,82–84].

Furthermore, environmental factors such as NaCl concentration and iron availability have been shown to significantly increase biofilm production in different strains of *P. salmonis* [85]. Consequently, strategies aimed at disrupting biofilm formation represent an important target for SRS control. The inhibitory effect observed for ChS at a MIC (1500 µg/mL) is consistent with previous reports describing the antimicrobial and anti-biofilm properties of sulfur-modified chitosans. Interestingly, the lack of inhibition at 750 µg/mL of ChS (sub-MIC) after 4 days of exposure could reflect a phenomenon frequently observed with antimicrobial compounds, where sub-MIC levels can stimulate bacterial adhesion, biofilm formation (Figure 8), or stress responses, rather than inhibit them. In the case of *P. salmonis*, exposure to natural substances (phytogenic feed additives), at subinhibitory levels, has been shown to modulate the expression of genes related to stress and biofilm formation, indicating that low concentrations of antimicrobials can activate adaptive responses in the bacteria to increase biofilm [86].

This phenomenon has also been described for licensed antibiotics such as FF, where exposure to sub-MIC levels in *P. salmonis* influences biofilm formation and the expression of virulence genes, depending on the strain and surface material [9,84]. Other results demonstrated that sub-MIC dilutions of FF significantly modulated the expression of the efflux pump acrAB and two components of the system, cpxAR and qseBC, as well as florfenicol resistance genes (tclor/tflor and t.flor) in *P. salmonis* isolates embedded in analyzed biofilms [87]. Therefore, the increase in biofilm observed at 750 µg/mL in the present study probably reflects a stress-induced response that promotes bacterial adhesion or EPS production in the extracellular matrix. This background information underscores the importance of the proper management and responsible use of authorized antimicrobials and emerging antimicrobial alternatives.

The information described above regarding the results obtained contributes to supporting the hypothesis that the chemical modification of chitosan with sulfate groups generated a biomimetic HS receptor with a greater affinity for the cell membrane of Gram-negative bacteria and increased its capacity to destabilize the membrane of *P. salmonis* and the reduction in biofilm formation. Also, due to the lack of scientific background on the exposure of *P. salmonis* to ChS and other chitosans, the data obtained in this study is the first results reported with a biomimetic biopolymer of HS, as an antibacterial alternative against this important pathogen of Chilean aquaculture.

© 2026 by the author(s). Distributed under a Creative Commons CC BY license.

Preprints.org (www.preprints.org) | NOT PEER-REVIEWED | Posted: 1 April 2026 doi:10.20944/preprints202604.0022.v1

Additionally, the biodegradable and biocompatible nature of chitosan makes it an attractive candidate for environmentally sustainable applications. Furthermore, in vivo studies and salmonid infection models are necessary to evaluate its therapeutic applications and its use alongside approved antimicrobials for synergistic control and the safety of these materials under aquaculture conditions. This is due to the risk of bacterial resistance and the environmental impact of frequently using antimicrobials to treat and control SRS [3,7,10,87]. The degree of sulfation (DS ≈ 0.92–0.95) also indicates that the chitosan has undergone significant chemical modification, which could boost its antimicrobial properties by raising its charge density and enhancing its interaction with bacterial membranes.

Therefore, further studies evaluating in vivo biocompatibility are required to assess the safety of the biomaterial. Overall, these findings improve our understanding of the structure-function relationships of modified chitosan derivatives, highlighting their potential role in developing sustainable antimicrobial strategies for aquaculture within a One Health approach.

5. Materials and Methods

5.1. Degree of Sulfation (DS) Estimation

The degree of sulfation (DS) of ChS was estimated from elemental composition obtained by energy-dispersive X-ray spectroscopy (EDS). The calculation was based on the sulfur-to-nitrogen (S/N) weight ratio, if each glucosamine unit in native chitosan contains one free amino group.

The DS was calculated according to the following equation adapted from previously reported sulfated chitosan studies:

$$\boldsymbol{DS = \frac{(S/N)}{(S/N) + k}}$$

where S and N represent the weight percentages of sulfur and nitrogen obtained from the EDS analysis, and k is a proportionality constant derived from the molecular composition of the glucosamine monomer. Elemental analysis using EDS revealed sulfur and nitrogen contents of 10.1 and 4.8 wt.-%, respectively, for the ChS sample. Based on these values, the degree of sulfation (DS) was calculated using two independent approaches. The DS was determined to be 0.95 using the sulfur-to-nitrogen ratio method, while the molar ratio approach yielded a similar value of 0.92, confirming the consistency of the calculation. These results suggest a significant increase in DS, indicating that most of the available amino or hydroxyl groups in the glucosamine units were substituted by sulphate groups. Theoretical sulfur content estimated from the calculated DS values ranged between 12.6% and 12.8%, which is slightly higher than the experimental value obtained by EDS (10.1%).

Elemental composition of the ChS was analyzed using energy-dispersive X-ray spectroscopy (EDS) coupled to the SEM system (Brand: JEOL, Model: JSM-IT300). Spectra were obtained from multiple regions of each sample to determine the relative abundance of carbon, oxygen, nitrogen, and sulfur. The presence of sulfur confirmed the successful incorporation of sulfate groups into the chitosan structure. Because EDS provides semi-quantitative elemental measurements, the DS value obtained should be considered an approximate estimation of the substitution level.

5.2. Structural and Morphological Characterization of ChS

Fourier Transform Infrared Spectroscopy (FTIR): Chemical modification of chitosan was confirmed by Fourier-transform infrared spectroscopy (FTIR). ChS samples were mixed with potassium bromide (KBr) and compressed into pellets prior to analysis. Spectra were recorded using a Thermo Nicolet iS50 spectrometer over a spectral range of 4000–400 cm^{-1} with a resolution of 4 cm^{-1}. Characteristic absorption bands associated with ChS were identified, including peaks at 1260 cm^{-1}, corresponding to asymmetric stretching of sulfate groups (S=O), and 1040 cm^{-1}, attributed to C–O–S vibrations. These signals confirmed the incorporation of sulfate groups into the chitosan backbone, mainly at the C2 and C6 positions of the glucosamine units.

© 2026 by the author(s). Distributed under a Creative Commons CC BY license.

Preprints.org (www.preprints.org) | NOT PEER-REVIEWED | Posted: 1 April 2026 doi:10.20944/preprints202604.0022.v1

5.3. Scanning Electron Microscopy (SEM) of Polymer

Surface morphology of the polymer and bacterial samples was examined using scanning electron microscopy (SEM). Samples were mounted on aluminum stubs and coated with a thin gold–palladium layer using a sputter coater to improve conductivity. Images were acquired using a JEOL JSM-IT300 scanning electron microscope operating at an accelerating voltage between 10–15 kV. Morphological features including particle size, aggregation state, and surface roughness were evaluated. The average particle size of the ChS ranged between 1 and 3 μm.

a. Biopolymer Preparation

ChS solutions were prepared at concentrations ranging from 31 to 3000 μg/mL in sterile phosphate-buffered saline (PBS, pH 7.4). The ChS had a molecular weight of 70 kDa and a degree of deacetylation of >75% and a zeta potential (ζ) value of -22 mV [16]. The ChC used as a control had a molecular weight of 70 kDa and a degree of deacetylation of 75%, according to the manufacturer's instructions (ALDRICH®), and was solubilized in a 1% acetic acid solution [14]. Sterile 10 mg/mL stock solutions of both biopolymers were prepared and filtered through 0.22 μm membranes (Startech®). Given the importance of this variable in the antibacterial effect of these polymers, the pH of both the culture medium and the final solutions was measured.

b. Antibacterial Activity Assays

The antibacterial activity of ChS against *P. salmonis* was evaluated using the microdilution method described in CLSI M07 (corresponding to the same methodology described in ISO 20776-1), with modifications adapted for slow-growing fish pathogens [88].

Bacterial Culture: The *P. salmonis* strain from genogroup LF-89 was donated by the Institute of Nutrition and Food Technology, University of Chile, Santiago, Chile. *P. salmonis* strain LF-89 was cultured in Austral-SRS medium prepared in the laboratory, as described by the authors and supplemented with 1% NaCl and 0.1% L-cysteine **[89,90]**. Cultures were incubated at 18 °C with gentle agitation (150 rpm) until reaching the logarithmic growth phase (OD630 ≈ 0.2). Bacterial suspensions were then adjusted to approximately (0.5 McFarland standard, 1.5 × 10^{-1}/mL) for all assays.

c. Minimum Inhibitory Concentration (MIC)

The MIC of ChS against *P. salmonis* was determined using the broth microdilution method. Serial two-fold dilutions (1:2) of ChS and commercial chitosan (ChC) were prepared. The concentration range tested in the assay was 46.9–6000 μg/mL.

Antimicrobial susceptibility assays were carried out in sterile 96-well microtiter plates. Each well contained: 155 μL of fresh Austral-SRS, 25 μL of the corresponding compound dilution, 20 μL of bacterial inoculum. The bacterial inoculum was adjusted to 0.5 McFarland turbidity standard. The final volume in each well was 200 μL. The plates were incubated at 18 °C with constant agitation (150 rpm) for 144 h.

In addition to the evaluated polymers, reference antimicrobial agents commonly used for the treatment of piscirickettsiosis were included as comparative controls, specifically: oxytetracycline, florfenicol and ChC was also tested under the same conditions to compare its antimicrobial activity with that of ChS. The following internal controls were included in each microplate: Growth control (culture medium + bacterial inoculum without antimicrobial compound), sterility control (culture medium without bacteria) and polymer blank (turbidity controls ChS and ChC without bacteria).

Bacterial growth was initially evaluated visually by turbidity and subsequently confirmed by optical density (OD) measurement using a microplate reader. When required, OD values were corrected by subtracting the OD of the sterile medium and OD turbidity controls. Also, by culture in Austral-SRS medium, from those wells where no growth was observed.

The MIC was defined as the lowest concentration compound that prevented visible bacterial growth and showed minimal OD relative to growth control. All experiments were performed in three independent biological replicates (n = 3).

© 2026 by the author(s). Distributed under a Creative Commons CC BY license.

Preprints.org (www.preprints.org) | NOT PEER-REVIEWED | Posted: 1 April 2026 doi:10.20944/preprints202604.0022.v1

5.4. Minimum Bactericidal Concentration (MBC)

To determine the minimum bactericidal concentration, aliquots from wells showing no visible growth were seeded in Austral-SRS medium and incubated for 14 days at 18 °C. The MBC was defined as the lowest concentration at which no bacterial colonies were observed.

5.5. Biofilm Inhibition Assay

Biofilm formation by *P. salmonis* exposed to ChS was evaluated with protocol described by Santibañez et al. **[85]** was used, with some modifications. The bacteria were cultured in sterile, 96-well, flat-bottom polystyrene microplates (JET BIOFIL). Austral-SRS medium was used, prepared in the same manner as for obtaining the MIC in this study. All wells had a final volume of 200 µL, prepared as follows: each control inoculum well was first filled with 180 µL of sterile Austral-SRS medium, while the Ch-S treatment wells were filled with 180 µL of a solution containing two Ch-S concentrations: the MIC (1500 µg/mL) and a sub-MIC (750 µg/mL), using the same sterile Austral-SRS medium as the solvent.

Similarly, the control antibiotic (oxytetracycline) was added to the corresponding wells in a solution volume of 180 µL, at a concentration of 5 µg/mL (slightly higher than the MIC of the bacterial strain (3.9 µg/mL) to provide positive antibiofilm control. Once all the microplates contained the volumes described above, the volume was brought up to 200 µL with 20 µL of bacterial inoculum (0.5 McFarland standard, 1.5×10^{-1}/mL) per well.

In addition, sterile Austral-SRS broth (200 µL) and ChS solution (200 µL) without inoculum at the two experimental concentrations (750 and 1500 µg/mL) were used as negative controls and to correct the OD_blanks measurements due to the increased background signal caused by the nonspecific interaction of the CV with polymeric matrices **[91,92]** like ChS. The microplates were capped and covered at the edges with permeable parafilm. They were incubated at 18 °C without shaking for up to 8 days.

Biofilm formation was quantified at 4, 6, and 8 days of culture by crystal violet (CV) staining, following a standardized protocols **[85,93]** with modifications. The volume of each well was discarded, and the plates were washed with 1x PBS by gentle pipetting. The plates were then allowed to dry at 37 °C for 30 min. Two hundred microliters of CV 0.1% were added to each well, and after 15 minutes of incubation, the CV solution was discarded. The wells were washed with sterile distilled water by slow, repeated pipetting to remove excess CV staining.

Next, they were dried at room temperature in an inverted position for 30 min. Then, the CV was solubilized by adding 200 µL of 96% ethanol for 10 minutes and measured at 595 nm using a microplate reader (BIO-RAD model 3550). Biofilm production was calculated according to the method of Stepanovic et al. **[93]**, using a proposed OD cutoff value (DOc): DOc will be defined as three standard deviations (SD) above the mean OD of the negative control (sterile medium): DOc = DOn + 3 × SD. DOn is the mean OD of the negative control and SD is its standard deviation. Therefore, the OD value of an analyzed strain will be expressed as the mean OD value of the strain or condition, reduced by the DOc value. The DOc value will be calculated separately for each microtiter plate. A negative value will be represented as zero (0), while any positive value will indicate biofilm production. The percentage of biofilm inhibition was calculated using the equation:

$$\text{Biofilm inhibition (\%)} = \left(\mathbf{1} - \frac{\boldsymbol{A}_{\text{treated}}}{\boldsymbol{A}_{\text{control}}}\right) \times \mathbf{100}$$

All experiments were performed in three independent biological replicates.

5.6. Bacterial Viability and Membrane Permeability by Fluorescence Microscopy (LIVE/DEAD Imaging)

Membrane integrity of P. salmonis cells exposed to ChS was evaluated using the LIVE/DEAD BacLight bacterial viability kit (Thermo Fisher Scientific, USA). Bacterial suspensions (0.5 McFarland standard, 1.5×10^{-1}/mL) were exposed to ChS at its MIC (1500 µg/mL) and the same culture without polymers was used as a negative control, and ethanol at 50% concentration was used with the culture as a positive control for cell membrane alteration [94]. and incubated at 18 °C with agitation (150

© 2026 by the author(s). Distributed under a Creative Commons CC BY license.

Preprints.org (www.preprints.org) | NOT PEER-REVIEWED | Posted: 1 April 2026 doi:10.20944/preprints202604.0022.v1

rpm). Samples were stained with SYTO9 (6 μM) and PI (30 μM) following the manufacturer's instructions and based on previous reports [73]. Samples were taken for vital staining at 10 min, 30 min, 1 hour, 5 hours, 24 hours, 48 hours, 72 hours, 96 hours, and 120 hours of experimental exposure to the polymers and controls. Following experimental exposure to the biopolymers, the samples analyzed using the fluorescence ratio assay were subsequently cultured in Austral-SRS medium to evaluate bacterial recovery after 120 hours of incubation with the treatments.

Fluorescence images were obtained using a Zeiss LSM 800 confocal laser scanning microscope with excitation wavelengths of 488 nm (SYTO9) and 561 nm (PI). Image analysis was performed using ImageJ software to quantify fluorescence intensity. Green fluorescence corresponded to cells with intact membranes, while red fluorescence indicated compromised membranes. Changes in permeability in bacterial cell membrane were expressed as the Green/Red fluorescence ratio.

5.7. Scanning Electron Microscopy (SEM) of Bacteria

Morphostructural analysis was carried out using a Microscope (JEOL instrument model JSM-IT300LV, Pleasanton, CA, USA) located at the Faculty of Dentistry of the University of Chile. To examine by SEM imagens the changes in the morphology of bacteria exposed to biopolymers, samples were taken from bacterial cultures of *P. salmonis* exposed to ChS, ChC and from the culture without exposure to the polymers as a control. Before evaluation, the samples were lyophilized and metallized with gold, according to methods previously described **[95]**.

5.8. Statistical Analysis

All experiments were performed in triplicate. Results are expressed as mean ± standard deviation (SD) and in the case of corrected OD in biofilm measurement tests, the standard error of the mean was used. Statistical significance between treatments was determined using one-way analysis of variance (ANOVA) followed by Tukey's post hoc test using GraphPad Prism version 9.0. Differences were considered statistically significant when $p < 0.05$.

6. Conclusions

This study demonstrates that ChS exhibits measurable antibacterial activity against *P. salmonis.* This is the first report on the in vitro antibacterial effects of sulfated chitosan on the permeability of the *P. salmonis* cell membrane, which is structurally similar to HS. Microanalysis using SEM-EDS confirmed the incorporation of sulfate groups into ChS with a degree of sulfation of 0.92-0.95 and likely contributed to the observed antimicrobial activity against *P. salmonis*, as antibacterial assays showed that ChS increased membrane permeability at lower concentrations than ChC. This suggests that sulfation enhances the antimicrobial properties of the chitosan polymer.

Fluorescence-based studies of membrane alteration revealed a progressive change ($p < 0.05$) in permeability in bacterial cell membrane following exposure to ChS, associated with increased membrane permeability. Microscopy-fluorescence observations further demonstrated the formation of bacterial aggregates and extensive damage to the bacterial envelope. These findings were supported by SEM, which revealed severe morphological alterations including surface irregularities, cell aggregation, loss of normal morphology, also significant decrease ($p < 0.05$) in biofilm at the MIC during periods of greatest exposure (6 and 8 days), according to the CV staining method.

Further research is also recommended into the synergistic effects of ChS and authorized antibiotics in other *P. salmonis* strains, as well as on other virulence factors, using in vitro and in vivo assays. Ultimately, despite having lower intrinsic potency than licensed antibiotics, the biodegradable and biomimetic nature of ChS highlights its potential as a complementary antimicrobial biomaterial. This provides a more sustainable approach to controlling bacterial infections in aquaculture within the One Health framework.

© 2026 by the author(s). Distributed under a Creative Commons CC BY license.

Preprints.org (www.preprints.org) | NOT PEER-REVIEWED | Posted: 1 April 2026 doi:10.20944/preprints202604.0022.v1

Author Contributions: Conceptualization, S.A.B., A.A.H. and A.N.-C.; methodology, S.A.B., D.A.M.; software, S.A.B.; validation, S.A.B. and A.N.-C.; formal analysis, S.A.B. and A.N.-C.; investigation, S.A.B. and D.A.M.; resources, A.A.H. and A.N.-C.; data curation, D.A.M.; writing—original draft preparation, S.A.B. and D.A.M.; writing—review and editing, S.A.B. and A.N.-C.; visualization, S.A.B., D.A.M.; supervision, S.A.B. and A.N.-C.; project administration, S.A.B.; funding acquisition, A.A.H. and A.N.-C. All authors have read and agreed to the published version of the manuscript.

Funding: This research received no external funding.

Institutional Review Board Statement: Not applicable.

Informed Consent Statement: Not applicable.

Data Availability Statement: The data presented in this study are available on request from the corresponding author.

Acknowledgments: A. N.-C. thanks the ANID for financial support through Regular Fondecyt Project No. 1250931, which partially funded this work. PhD student, D. Arrieta is grateful for the funding provided by program Doctorate in Forestry, Agricultural and Veterinary Sciences, University of Chile, for the fee exemption scholarship from this accredited program.

Conflicts of Interest: The authors declare no conflicts of interest.

References

1. Rozas-Serri, M. Why Does Piscirickettsia Salmonis Break the Immunological Paradigm in Farmed Salmon? Biological Context to Understand the Relative Control of Piscirickettsiosis. *Front. Immunol.* **2022**, *13*, 856896, doi:10.3389/fimmu.2022.856896.
2. Price, D.; Sánchez, J.; McClure, J.; McConkey, S.; Ibarra, R.; St-Hilaire, S. Assessing Concentration of Antibiotics in Tissue during Oral Treatments against Piscirickettsiosis. *Preventive Veterinary Medicine* **2018**, *156*, 16–21, doi:10.1016/j.prevetmed.2018.04.014.
3. Diethelm-Varela, B.; Atero, N.; Córdova-Bührle, F.; Rezende, E.L.; Gelcich, S.; Sandoval, O.; Navarro, C.; Mardones, F.O. Epidemiology of Salmonid Rickettsial Septicemia (SRS) in Farmed Salmon: The Role of Sea Lice Infestations in Mortality Risk. *Journal of Fish Diseases* **2025**, e70097, doi:10.1111/jfd.70097.
4. Cabello, F.C.; Godfrey, H.P.; Tomova, A.; Ivanova, L.; Dölz, H.; Millanao, A.; Buschmann, A.H. Antimicrobial Use in Aquaculture Re-examined: Its Relevance to Antimicrobial Resistance and to Animal and Human Health. *Environmental Microbiology* **2013**, *15*, 1917–1942, doi:10.1111/1462-2920.12134.
5. Millanao, A.R.; Barrientos-Schaffeld, C.; Siegel-Tike, C.D.; Tomova, A.; Ivanova, L.; Godfrey, H.P.; Dölz, H.J.; Buschmann, A.H.; Cabello, F.C. Resistencia a Los Antimicrobianos En Chile y El Paradigma de Una Salud: Manejando Los Riesgos Para La Salud Pública Humana y Animal Resultante Del Uso de Antimicrobianos En La Acuicultura Del Salmón y En Medicina. *Rev. chil. infectol.* **2018**, *35*, 299–308, doi:10.4067/s0716-10182018000300299.
6. Souto Cavalli, L.; Tapia-Jopia, C.; Ochs, C.; López Gómez, M.A.; Neis, B. Salmon Mass Mortality Events and Occupational Health and Safety in Chilean Aquaculture. *All Life* **2023**, *16*, 2207772, doi:10.1080/26895293.2023.2207772.
7. Farias, D.R.; Ibarra, R.; Tucca, F.; Jaramillo-Torres, A.; Cornejo, J.; Ibieta, P.; Mardones, F.O.; Avendaño-Herrera, R. Insights and Lessons from Chilean Salmon Aquaculture on Antimicrobial Use. *Antibiotics* **2025**, *14*, 1177, doi:10.3390/antibiotics14121177.
8. Rozas, M.; Enríquez, R. Piscirickettsiosis and *P Iscirickettsia Salmonis* in Fish: A Review. *Journal of Fish Diseases* **2014**, *37*, 163–188, doi:10.1111/jfd.12211.
9. Oliver, C.; Céspedes, C.; Santibañez, N.; Ruiz, P.; Romero, A. Subinhibitory Concentrations of Florfenicol Increase the Biofilm Formation of *Piscirickettsia Salmonis*. *Journal of Fish Diseases* **2023**, *46*, 591–596, doi:10.1111/jfd.13757.

© 2026 by the author(s). Distributed under a Creative Commons CC BY license.

Preprints.org (www.preprints.org) | NOT PEER-REVIEWED | Posted: 1 April 2026 doi:10.20944/preprints202604.0022.v1

10. San Martín, B.; Fresno, M.; Cornejo, J.; Godoy, M.; Ibarra, R.; Vidal, R.; Araneda, M.; Anadón, A.; Lapierre, L. Optimization of Florfenicol Dose against Piscirickettsia Salmonis in Salmo Salar through PK/PD Studies. *PLoS ONE* **2019**, *14*, e0215174, doi:10.1371/journal.pone.0215174.
11. Bondad-Reantaso, M.G.; MacKinnon, B.; Karunasagar, I.; Fridman, S.; Alday-Sanz, V.; Brun, E.; Le Groumellec, M.; Li, A.; Surachetpong, W.; Karunasagar, I.; et al. Review of Alternatives to Antibiotic Use in Aquaculture. *Reviews in Aquaculture* **2023**, *15*, 1421–1451, doi:10.1111/raq.12786.
12. Valcarcel, J.; Novoa-Carballal, R.; Pérez-Martín, R.I.; Reis, R.L.; Vázquez, J.A. Glycosaminoglycans from Marine Sources as Therapeutic Agents. *Biotechnology Advances* **2017**, *35*, 711–725, doi:10.1016/j.biotechadv.2017.07.008.
13. Arrieta-Mendoza, D.; Garces, B.; Hidalgo, A.A.; Neira, V.; Ramirez, G.; Neira-Carrillo, A.; Bucarey, S.A. Design of a New Vaccine Prototype against Porcine Circovirus Type 2 (PCV2), M. Hyopneumoniae and M. Hyorhinis Based on Multiple Antigens Microencapsulation with Sulfated Chitosan. *Vaccines* **2024**, *12*, 550, doi:10.3390/vaccines12050550.
14. Jiménez-Arriagada, D.; Hidalgo, A.A.; Neira, V.; Neira-Carrillo, A.; Bucarey, S.A. Low Molecular Weight Sulfated Chitosan Efficiently Reduces Infection Capacity of Porcine Circovirus Type 2 (PCV2) in PK15 Cells. *Virol J* **2022**, *19*, 52, doi:10.1186/s12985-022-01781-7.
15. Bucarey, S.A.; Ramos, V.; Hidalgo, A.A.; Neira, V.; Neira-Carrillo, A.; Ferrer, P. Low-Molecular-Weight Sulfated Chitosan Microparticles Efficiently Bind HIV-1 In Vitro: Potential for Microbicide Applications. *Molecules* **2026**, *31*, 395, doi:10.3390/molecules31030395.
16. Bucarey Vivanco, S.A.; Neira Carrillo, A.; Neira Ramirez, V.M. US20210059951 Vaccine Treatment and Control Infectious against Viral Pathogens Utilizing Heparan Sulfate (HS) as Cellular Receptor. 2022.
17. Sahariah, P.; Másson, M. Antimicrobial Chitosan and Chitosan Derivatives: A Review of the Structure–Activity Relationship. *Biomacromolecules* **2017**, *18*, 3846–3868, doi:10.1021/acs.biomac.7b01058.
18. Dimassi, S.; Tabary, N.; Chai, F.; Blanchemain, N.; Martel, B. Sulfonated and Sulfated Chitosan Derivatives for Biomedical Applications: A Review. *Carbohydrate Polymers* **2018**, *202*, 382–396, doi:10.1016/j.carbpol.2018.09.011.
19. Doncel-Pérez, E.; Aranaz, I.; Bastida, A.; Revuelta, J.; Camacho, C.; Acosta, N.; Garrido, L.; Civera, C.; García-Junceda, E.; Heras, A.; et al. Synthesis, Physicochemical Characterization and Biological Evaluation of Chitosan Sulfate as Heparan Sulfate Mimics. *Carbohydrate Polymers* **2018**, *191*, 225–233, doi:10.1016/j.carbpol.2018.03.036.
20. Cesari, A.; Fabiano, A.; Piras, A.M.; Zambito, Y.; Uccello-Barretta, G.; Balzano, F. Binding and Mucoadhesion of Sulfurated Derivatives of Quaternary Ammonium-Chitosans and Their Nanoaggregates: An NMR Investigation. *Journal of Pharmaceutical and Biomedical Analysis* **2020**, *177*, 112852, doi:10.1016/j.jpba.2019.112852.
21. Revuelta, J.; Fraile, I.; Monterrey, D.T.; Peña, N.; Benito-Arenas, R.; Bastida, A.; Fernández-Mayoralas, A.; García-Junceda, E. Heparanized Chitosans: Towards the Third Generation of Chitinous Biomaterials. *Mater. Horiz.* **2021**, *8*, 2596–2614, doi:10.1039/D1MH00728A.
22. Žigrayová, D.; Mikušová, V.; Mikuš, P. Advances in Chitosan Derivatives: Preparation, Properties and Applications in Pharmacy and Medicine. *Gels* **2024**, *10*, 701, doi:10.3390/gels10110701.
23. Federer, C.; Kurpiers, M.; Bernkop-Schnürch, A. Thiolated Chitosans: A Multi-Talented Class of Polymers for Various Applications. *Biomacromolecules* **2021**, *22*, 24–56, doi:10.1021/acs.biomac.0c00663.
24. Muñoz-Bonilla, A.; Echeverria, C.; Sonseca, Á.; Arrieta, M.P.; Fernández-García, M. Bio-Based Polymers with Antimicrobial Properties towards Sustainable Development. *Materials* **2019**, *12*, 641, doi:10.3390/ma12040641.
25. Ke, C.-L.; Deng, F.-S.; Chuang, C.-Y.; Lin, C.-H. Antimicrobial Actions and Applications of Chitosan. *Polymers* **2021**, *13*, 904, doi:10.3390/polym13060904.
26. Si, Z.; Hou, Z.; Vikhe, Y.S.; Thappeta, K.R.V.; Marimuthu, K.; De, P.P.; Ng, O.T.; Li, P.; Zhu, Y.; Pethe, K.; et al. Antimicrobial Effect of a Novel Chitosan Derivative and Its Synergistic Effect with Antibiotics. *ACS Appl. Mater. Interfaces* **2021**, *13*, 3237–3245, doi:10.1021/acsami.0c20881.

© 2026 by the author(s). Distributed under a Creative Commons CC BY license.

Preprints.org (www.preprints.org) | NOT PEER-REVIEWED | Posted: 1 April 2026 doi:10.20944/preprints202604.0022.v1

27. Kong, M.; Chen, X.G.; Xing, K.; Park, H.J. Antimicrobial Properties of Chitosan and Mode of Action: A State of the Art Review. *International Journal of Food Microbiology* **2010**, *144*, 51–63, doi:10.1016/j.ijfoodmicro.2010.09.012.
28. Muñoz-Bonilla, A.; Fernández-García, M. Polymeric Materials with Antimicrobial Activity. *Progress in Polymer Science* **2012**, *37*, 281–339, doi:10.1016/j.progpolymsci.2011.08.005.
29. Ke, C.-L.; Deng, F.-S.; Chuang, C.-Y.; Lin, C.-H. Antimicrobial Actions and Applications of Chitosan. *Polymers* **2021**, *13*, 904, doi:10.3390/polym13060904.
30. Egorov, A.R.; Kirichuk, A.A.; Rubanik, V.V.; Rubanik, V.V.; Tskhovrebov, A.G.; Kritchenkov, A.S. Chitosan and Its Derivatives: Preparation and Antibacterial Properties. *Materials* **2023**, *16*, 6076, doi:10.3390/ma16186076.
31. Laanoja, J.; Sihtmäe, M.; Vija, H.; Kurvet, I.; Otsus, M.; Šmits, K.; Kahru, A.; Kasemets, K. Particle-Driven Synergistic Antibacterial Effect of Silver–Chitosan Nanocomposites Against *Escherichia Coli* , *Pseudomonas Aeruginosa* , and *Staphylococcus Aureus*. *ACS Omega* **2025**, *10*, 27904–27919, doi:10.1021/acsomega.5c01067.
32. Raafat, D.; Sahl, H. Chitosan and Its Antimicrobial Potential – a Critical Literature Survey. *Microbial Biotechnology* **2009**, *2*, 186–201, doi:10.1111/j.1751-7915.2008.00080.x.
33. Yan, D.; Li, Y.; Liu, Y.; Li, N.; Zhang, X.; Yan, C. Antimicrobial Properties of Chitosan and Chitosan Derivatives in the Treatment of Enteric Infections. *Molecules* **2021**, *26*, 7136, doi:10.3390/molecules26237136.
34. Helander, I.M.; Nurmiaho-Lassila, E.-L.; Ahvenainen, R.; Rhoades, J.; Roller, S. Chitosan Disrupts the Barrier Properties of the Outer Membrane of Gram-Negative Bacteria. *International Journal of Food Microbiology* **2001**, *71*, 235–244, doi:10.1016/S0168-1605(01)00609-2.
35. Khalid, S.; Piggot, T.J.; Samsudin, F. Atomistic and Coarse Grain Simulations of the Cell Envelope of Gram-Negative Bacteria: What Have We Learned? *Acc. Chem. Res.* **2019**, *52*, 180–188, doi:10.1021/acs.accounts.8b00377.
36. Feng, P.; Luo, Y.; Ke, C.; Qiu, H.; Wang, W.; Zhu, Y.; Hou, R.; Xu, L.; Wu, S. Chitosan-Based Functional Materials for Skin Wound Repair: Mechanisms and Applications. *Front. Bioeng. Biotechnol.* **2021**, *9*, 650598, doi:10.3389/fbioe.2021.650598.
37. Dasagrandhi, C.; Park, S.; Jung, W.-K.; Kim, Y.-M. Antibacterial and Biofilm Modulating Potential of Ferulic Acid-Grafted Chitosan against Human Pathogenic Bacteria. *IJMS* **2018**, *19*, 2157, doi:10.3390/ijms19082157.
38. Wrońska, N.; Katir, N.; Miłowska, K.; Hammi, N.; Nowak, M.; Kędzierska, M.; Anouar, A.; Zawadzka, K.; Bryszewska, M.; El Kadib, A.; et al. Antimicrobial Effect of Chitosan Films on Food Spoilage Bacteria. *IJMS* **2021**, *22*, 5839, doi:10.3390/ijms22115839.
39. Niu, B.; Zhang, G. Effects of Different Nanoparticles on Microbes. *Microorganisms* **2023**, *11*, 542, doi:10.3390/microorganisms11030542.
40. Marshall, S.H.; Gómez, F.A.; Ramírez, R.; Nilo, L.; Henríquez, V. Biofilm Generation by Piscirickettsia Salmonis under Growth Stress Conditions: A Putative in Vivo Survival/Persistence Strategy in Marine Environments. *Research in Microbiology* **2012**, *163*, 557–566, doi:10.1016/j.resmic.2012.08.002.
41. Manik, E.R.; Kaban, J. Synthesis of Sulfated Chitosan Through Sulfation Reaction of Chitosan with Chlorosulfonic Acid in N, N-Dimethylformamide, and Antibacterial Activity Test. *JCNaR* **2022**, *4*, 1–8, doi:10.32734/jcnar.v4i1.9353.
42. Sun, Z.; Shi, C.; Wang, X.; Fang, Q.; Huang, J. Synthesis, Characterization, and Antimicrobial Activities of Sulfonated Chitosan. *Carbohydrate Polymers* **2017**, *155*, 321–328, doi:10.1016/j.carbpol.2016.08.069.
43. Fatoni, A.; Ahmad, I.N.; Utami, H.; Erjon; Rendowaty, A.; Hidayati, N. Synthesis, Characterization of Chitosan Sulfate Nanoparticles and Their Activity against Bacterial.; Bogor, Indonesia, 2023; p. 020007.
44. Ardean, C.; Davidescu, C.M.; Nemeş, N.S.; Negrea, A.; Ciopec, M.; Duteanu, N.; Negrea, P.; Duda-Seiman, D.; Musta, V. Factors Influencing the Antibacterial Activity of Chitosan and Chitosan Modified by Functionalization. *IJMS* **2021**, *22*, 7449, doi:10.3390/ijms22147449.
45. Mania, S.; Banach-Kopeć, A.; Staszczyk, K.; Kulesza, J.; Augustin, E.; Tylingo, R. An Influence of Molecular Weight, Deacetylation Degree of Chitosan Xerogels on Their Antimicrobial Activity and Cytotoxicity. Comparison of Chitosan Materials Obtained Using Lactic Acid and CO2 Saturation. *Carbohydrate Research* **2023**, *534*, 108973, doi:10.1016/j.carres.2023.108973.

© 2026 by the author(s). Distributed under a Creative Commons CC BY license.

Preprints.org (www.preprints.org) | NOT PEER-REVIEWED | Posted: 1 April 2026 doi:10.20944/preprints202604.0022.v1

46. Sila, A.; Bougatef, H.; Capitani, F.; Krichen, F.; Mantovani, V.; Amor, I.B.; Galeotti, F.; Maccari, F.; Nedjar, N.; Volpi, N.; et al. Studies on European Eel Skin Sulfated Glycosaminoglycans: Recovery, Structural Characterization and Anticoagulant Activity. *International Journal of Biological Macromolecules* **2018**, *115*, 891–899, doi:10.1016/j.ijbiomac.2018.04.125.
47. Revuelta, J.; Rusu, L.; Frances-Gomez, C.; Trapero, E.; Iglesias, S.; Pinilla, E.C.; Blázquez, A.-B.; Gutiérrez-Adán, A.; Konuparamban, A.; Moreno, O.; et al. Synthetic Heparan Sulfate Mimics Based on Chitosan Derivatives Show Broad-Spectrum Antiviral Activity. *Commun Biol* **2025**, *8*, 360, doi:10.1038/s42003-025-07763-z.
48. Maïza, A.; Chantepie, S.; Vera, C.; Fifre, A.; Huynh, M.B.; Stettler, O.; Ouidja, M.O.; Papy-Garcia, D. The Role of Heparan Sulfates in Protein Aggregation and Their Potential Impact on Neurodegeneration. *FEBS Letters* **2018**, *592*, 3806–3818, doi:10.1002/1873-3468.13082.
49. Ferreira, A.; Royaux, I.; Liu, J.; Wang, Z.; Su, G.; Moechars, D.; Callewaert, N.; De Muynck, L. The 3-O Sulfation of Heparan Sulfate Proteoglycans Contributes to the Cellular Internalization of Tau Aggregates. *BMC Mol and Cell Biol* **2022**, *23*, 61, doi:10.1186/s12860-022-00462-1.
50. Liao, Y.-E.; Liu, J.; Arnold, K. Heparan Sulfates and Heparan Sulfate Binding Proteins in Sepsis. *Front. Mol. Biosci.* **2023**, *10*, 1146685, doi:10.3389/fmolb.2023.1146685.
51. Khan, S.; Faisal, S.; Shams, D.F.; Zia, M.; Nadhman, A. Photo-inactivation of Bacteria in Hospital Effluent via Thiolated Iron-doped Nanoceria. *IET Nanobiotechnology* **2019**, *13*, 875–879, doi:10.1049/iet-nbt.2019.0149.
52. Schmitz, T.; Hombach, J.; Bernkop-Schnürch, A. Chitosan-N-Acetyl Cysteine Conjugates: In Vitro Evaluation of Permeation Enhancing and P-Glycoprotein Inhibiting Properties. *Drug Delivery* **2008**, *15*, 245–252, doi:10.1080/10717540802006708.
53. Rajan, A.; Robertson, M.J.; Carter, H.E.; Poole, N.M.; Clark, J.R.; Green, S.I.; Criss, Z.K.; Zhao, B.; Karandikar, U.; Xing, Y.; et al. Enteroaggregative E. Coli Adherence to Human Heparan Sulfate Proteoglycans Drives Segment and Host Specific Responses to Infection. *PLoS Pathog* **2020**, *16*, e1008851, doi:10.1371/journal.ppat.1008851.
54. Sanchez, H.; Hopkins, D.; Demirdjian, S.; Gutierrez, C.; O'Toole, G.A.; Neelamegham, S.; Berwin, B. Identification of Cell-Surface Glycans That Mediate Motility-Dependent Binding and Internalization of Pseudomonas Aeruginosa by Phagocytes. *Molecular Immunology* **2021**, *131*, 68–77, doi:10.1016/j.molimm.2020.12.012.
55. Zehr, E.P.; Erzen, C.L.; Oshima, K.; Langouet-Astrie, C.J.; LaRiviere, W.B.; Shi, D.; Zhang, F.; McCollister, B.D.; Windham, S.L.; Rizzo, A.N.; et al. Bacterial Pneumonia-Induced Shedding of Epithelial Heparan Sulfate Inhibits the Bactericidal Activity of Cathelicidin in a Murine Model. *American Journal of Physiology-Lung Cellular and Molecular Physiology* **2024**, *326*, L206–L212, doi:10.1152/ajplung.00178.2023.
56. Day, C.J.; Tran, E.N.; Semchenko, E.A.; Tram, G.; Hartley-Tassell, L.E.; Ng, P.S.K.; King, R.M.; Ulanovsky, R.; McAtamney, S.; Apicella, M.A.; et al. Glycan:Glycan Interactions: High Affinity Biomolecular Interactions That Can Mediate Binding of Pathogenic Bacteria to Host Cells. *Proc. Natl. Acad. Sci. U.S.A.* **2015**, *112*, doi:10.1073/pnas.1421082112.
57. Yeh, M.; Cheng, K.; Hu, C.; Huang, Y.; Young, J. Novel Protein-Loaded Chondroitin Sulfate–Chitosan Nanoparticles: Preparation and Characterization. *Acta Biomaterialia* **2011**, *7*, 3804–3812, doi:10.1016/j.actbio.2011.06.026.
58. Serizawa, T.; Yamaguchi, M.; Akashi, M. Alternating Bioactivity of Polymeric Layer-by-Layer Assemblies: Anticoagulation vs Procoagulation of Human Blood. *Biomacromolecules* **2002**, *3*, 724–731, doi:10.1021/bm0200027.
59. Keast, D.; Janmohammad, A. The Hemostatic and Wound Healing Effect of Chitosan Following Debridement of Chronic Ulcers. *Wounds* **2021**, *33*, 263–270, doi:10.25270/wnds/082421.01.
60. Riske, F.; Schroeder, J.; Belliveau, J.; Kang, X.; Kutzko, J.; Menon, M.K. The Use of Chitosan as a Flocculant in Mammalian Cell Culture Dramatically Improves Clarification Throughput without Adversely Impacting Monoclonal Antibody Recovery. *Journal of Biotechnology* **2007**, *128*, 813–823, doi:10.1016/j.jbiotec.2006.12.023.
61. Wang, W.; Xue, C.; Mao, X. Chitosan: Structural Modification, Biological Activity and Application. *International Journal of Biological Macromolecules* **2020**, *164*, 4532–4546, doi:10.1016/j.ijbiomac.2020.09.042.

© 2026 by the author(s). Distributed under a Creative Commons CC BY license.

Preprints.org (www.preprints.org) | NOT PEER-REVIEWED | Posted: 1 April 2026 doi:10.20944/preprints202604.0022.v1

62. Ojeda-Hernández, D.D.; Canales-Aguirre, A.A.; Matias-Guiu, J.A.; Matias-Guiu, J.; Gómez-Pinedo, U.; Mateos-Díaz, J.C. Chitosan–Hydroxycinnamic Acids Conjugates: Emerging Biomaterials with Rising Applications in Biomedicine. *IJMS* **2022**, *23*, 12473, doi:10.3390/ijms232012473.
63. Makshakova, O.N.; Zuev, Y.F. Interaction-Induced Structural Transformations in Polysaccharide and Protein-Polysaccharide Gels as Functional Basis for Novel Soft-Matter: A Case of Carrageenans. *Gels* **2022**, *8*, 287, doi:10.3390/gels8050287.
64. Holyavka, M.G.; Goncharova, S.S.; Sorokin, A.V.; Lavlinskaya, M.S.; Redko, Y.A.; Faizullin, D.A.; Baidamshina, D.R.; Zuev, Y.F.; Kondratyev, M.S.; Kayumov, A.R.; et al. Novel Biocatalysts Based on Bromelain Immobilized on Functionalized Chitosans and Research on Their Structural Features. *Polymers* **2022**, *14*, 5110, doi:10.3390/polym14235110.
65. Xia, Y.; Wang, D.; Liu, D.; Su, J.; Jin, Y.; Wang, D.; Han, B.; Jiang, Z.; Liu, B. Applications of Chitosan and Its Derivatives in Skin and Soft Tissue Diseases. *Front. Bioeng. Biotechnol.* **2022**, *10*, 894667, doi:10.3389/fbioe.2022.894667.
66. Zeng, K.; Groth, T.; Zhang, K. Recent Advances in Artificially Sulfated Polysaccharides for Applications in Cell Growth and Differentiation, Drug Delivery, and Tissue Engineering. *ChemBioChem* **2019**, *20*, 737–746, doi:10.1002/cbic.201800569.
67. Herrera, V.; Olavarría, N.; Saavedra, J.; Yuivar, Y.; Bustos, P.; Almarza, O.; Mancilla, M. Complete Lipopolysaccharide of Piscirickettsia Salmonis Is Required for Full Virulence in the Intraperitoneally Challenged Atlantic Salmon, Salmo Salar, Model. *Front. Cell. Infect. Microbiol.* **2022**, *12*, 845661, doi:10.3389/fcimb.2022.845661.
68. Oliver, C.; Sánchez, P.; Valenzuela, K.; Hernández, M.; Pontigo, J.P.; Rauch, M.C.; Garduño, R.A.; Avendaño-Herrera, R.; Yáñez, A.J. Subcellular Location of Piscirickettsia Salmonis Heat Shock Protein 60 (Hsp60) Chaperone by Using Immunogold Labeling and Proteomic Analysis. *Microorganisms* **2020**, *8*, 117, doi:10.3390/microorganisms8010117.
69. Oliver, C.; Hernández, M.A.; Tandberg, J.I.; Valenzuela, K.N.; Lagos, L.X.; Haro, R.E.; Sánchez, P.; Ruiz, P.A.; Sanhueza-Oyarzún, C.; Cortés, M.A.; et al. The Proteome of Biologically Active Membrane Vesicles from Piscirickettsia Salmonis LF-89 Type Strain Identifies Plasmid-Encoded Putative Toxins. *Front. Cell. Infect. Microbiol.* **2017**, *7*, 420, doi:10.3389/fcimb.2017.00420.
70. Valenzuela-Aviles, P.; Torrealba, D.; Figueroa, C.; Mercado, L.; Dixon, B.; Conejeros, P.; Gallardo-Matus, J. Why Vaccines Fail against Piscirickettsiosis in Farmed Salmon and Trout and How to Avoid It: A Review. *Front. Immunol.* **2022**, *13*, 1019404, doi:10.3389/fimmu.2022.1019404.
71. Gerlach, R.; Hensel, M. Protein Secretion Systems and Adhesins: The Molecular Armory of Gram-Negative Pathogens. *International Journal of Medical Microbiology* **2007**, *297*, 401–415, doi:10.1016/j.ijmm.2007.03.017.
72. Sánchez, P.; Oliver, C.; Hernández, M.; Cortés, M.; Cecilia Rauch, M.; Valenzuela, K.; Garduño, R.A.; Avendaño-Herrera, R.; Yáñez, A.J. In Vitro Genomic and Proteomic Evidence of a Type IV Pili-like Structure in the Fish Pathogen Piscirickettsia Salmonis. *FEMS Microbiology Letters* **2018**, *365*, doi:10.1093/femsle/fny169.
73. Levipan, H.A.; Irgang, R.; Opazo, L.F.; Araya-León, H.; Avendaño-Herrera, R. Collective Behavior and Virulence Arsenal of the Fish Pathogen Piscirickettsia Salmonis in the Biofilm Realm. *Front. Cell. Infect. Microbiol.* **2022**, *12*, 1067514, doi:10.3389/fcimb.2022.1067514.
74. Nag, M.; Lahiri, D.; Mukherjee, D.; Banerjee, R.; Garai, S.; Sarkar, T.; Ghosh, S.; Dey, A.; Ghosh, S.; Pattnaik, S.; et al. Functionalized Chitosan Nanomaterials: A Jammer for Quorum Sensing. *Polymers* **2021**, *13*, 2533, doi:10.3390/polym13152533.
75. Limayem, A.; Patil, S.B.; Mehta, M.; Cheng, F.; Nguyen, M. A Streamlined Study on Chitosan-Zinc Oxide Nanomicelle Properties to Mitigate a Drug-Resistant Biofilm Protection Mechanism. *Front. Nanotechnol.* **2020**, *2*, 592739, doi:10.3389/fnano.2020.592739.
76. Sahariah, P.; Papi, F.; Merz, K.L.; Sigurjonsson, O.E.; Meyer, R.L.; Nativi, C. Chitosan–Saccharide Conjugates for Eradication of *Pseudomonas Aeruginosa* Biofilms. *RSC Appl. Polym.* **2024**, *2*, 461–472, doi:10.1039/D3LP00263B.

© 2026 by the author(s). Distributed under a Creative Commons CC BY license.

Preprints.org (www.preprints.org) | NOT PEER-REVIEWED | Posted: 1 April 2026 doi:10.20944/preprints202604.0022.v1

77. Riahi, A.; Mabudi, H.; Tajbakhsh, E.; Roomiani, L.; Momtaz, H. Optimizing Chitosan Derived from Metapenaeus Affinis: A Novel Anti-Biofilm Agent against Pseudomonas Aeruginosa. *AMB Expr* **2024**, *14*, 77, doi:10.1186/s13568-024-01732-1.
78. Patel, K.K.; Surekha, D.B.; Tripathi, M.; Anjum, Md.M.; Muthu, M.S.; Tilak, R.; Agrawal, A.K.; Singh, S. Antibiofilm Potential of Silver Sulfadiazine-Loaded Nanoparticle Formulations: A Study on the Effect of DNase-I on Microbial Biofilm and Wound Healing Activity. *Mol. Pharmaceutics* **2019**, *16*, 3916–3925, doi:10.1021/acs.molpharmaceut.9b00527.
79. Huang, J.; Liu, Y.; Yang, L.; Zhou, F. Synthesis of Sulfonated Chitosan and Its Antibiofilm Formation Activity against E. Coli and S. Aureus. *International Journal of Biological Macromolecules* **2019**, *129*, 980–988, doi:10.1016/j.ijbiomac.2019.02.079.
80. Liu, Y.; Jiang, Y.; Zhu, J.; Huang, J.; Zhang, H. Inhibition of Bacterial Adhesion and Biofilm Formation of Sulfonated Chitosan against Pseudomonas Aeruginosa. *Carbohydrate Polymers* **2019**, *206*, 412–419, doi:10.1016/j.carbpol.2018.11.015.
81. Sun, J.; Shen, H.-L.; Pan, J.-N.; Yu, T.; Zhou, W.-W. Ferrous Sulfate/Carboxymethyl Chitosan Agar-Based Film Triggers Ferroptosis in Pseudomonas Aeruginosa Planktonic and Biofilm Cells for Antibacterial Preservation of Fruits and Vegetables. *International Journal of Biological Macromolecules* **2025**, *308*, 142697, doi:10.1016/j.ijbiomac.2025.142697.
82. Zúñiga, A.; Solis, C.; Cartes, C.; Nourdin, G.; Yañez, A.; Romero, A.; Haussmann, D.; Figueroa, J. Transcriptional Analysis of Metabolic and Virulence Genes Associated with Biofilm Formation in *Piscirickettsia Salmonis* Strains. *FEMS Microbiology Letters* **2020**, *367*, fnaa180, doi:10.1093/femsle/fnaa180.
83. Levipan, H.A.; Irgang, R.; Yáñez, A.; Avendaño-Herrera, R. Improved Understanding of Biofilm Development by Piscirickettsia Salmonis Reveals Potential Risks for the Persistence and Dissemination of Piscirickettsiosis. *Sci Rep* **2020**, *10*, 12224, doi:10.1038/s41598-020-68990-4.
84. Oliver, C.; Ruiz, P.; Vidal, J.M.; Carrasco, C.; Escalona, C.E.; Barros, J.; Sepúlveda, D.; Urrutia, H.; Romero, A. Effect of Florfenicol on *Piscirickettsia Salmonis* Biofilm Formed in Materials Used in Salmonid Nets, Nylon and HIGH-DENSITY Polyethylene. *Journal of Fish Diseases* **2024**, *47*, e13862, doi:10.1111/jfd.13862.
85. Santibañez, N.; Vega, M.; Pérez, T.; Yáñez, A.; González-Stegmaier, R.; Figueroa, J.; Enríquez, R.; Oliver, C.; Romero, A. Biofilm Produced In Vitro by Piscirickettsia Salmonis Generates Differential Cytotoxicity Levels and Expression Patterns of Immune Genes in the Atlantic Salmon Cell Line SHK-1. *Microorganisms* **2020**, *8*, 1609, doi:10.3390/microorganisms8101609.
86. Santibáñez, N.; Vega, M.; Pérez, T.; Enriquez, R.; Escalona, C.E.; Oliver, C.; Romero, A. In Vitro Effects of Phytogenic Feed Additive on *Piscirickettsia Salmonis* Growth and Biofilm Formation. *Journal of Fish Diseases* **2024**, *47*, e13913, doi:10.1111/jfd.13913.
87. Escalona, C.E.; Santibañez, N.; Cortés, M.; Arriagada, V.; Ruiz, P.; Fuentes, D.; Romero, A.; Oliver, C. Sub-Inhibitory Concentrations of Florfenicol Modulate the Expression of Biofilm Formation and Antibiotic Resistance-Associated Genes in Biofilm-Embedded *Piscirickettsia Salmonis*. *Journal of Fish Diseases* **2026**, e70166, doi:10.1111/jfd.70166.
88. SERNAPESCA: SERVICIO NACIONAL DE PESCA Y ACUICULTURA; DEPARTAMENTO DE SALUD ANIMAL Programa Sanitario General para la Vigilancia de la Susceptibilidad a Antimicrobianos en la Salmonicultura: Procedimiento de toma de muestras para aislamiento de Piscirickettsia salmonis y análisis para determinación de concentración mínima inhibitoria (CMI), mediante microdilución en caldo; NORMA TÉCNICA Nº4; Servicio Nacional de Pesca y Acuicultura (SERNAPESCA): Santiago, Chile, 2020; p. 16;.
89. Mikalsen, J.; SkjÃ¦rvik, O.; Wiik-Nielsen, J.; Wasmuth, M.A.; Colquhoun, D.J. Agar Culture of *Piscirickettsia Salmonis* , a Serious Pathogen of Farmed Salmonid and Marine Fish. *FEMS Microbiology Letters* **2008**, *278*, 43–47, doi:10.1111/j.1574-6968.2007.00977.x.
90. Vera, T.; Isla, A.; Cuevas, A.; Figueroa, J. Un Nuevo Medio de Cultivo Líquido Para El Patógeno Piscirickettsia Salmonis. *Arch. med. vet.* **2012**, *44*, 273–277, doi:10.4067/S0301-732X2012000300010.
91. Peeters, E.; Nelis, H.J.; Coenye, T. Comparison of Multiple Methods for Quantification of Microbial Biofilms Grown in Microtiter Plates. *Journal of Microbiological Methods* **2008**, *72*, 157–165, doi:10.1016/j.mimet.2007.11.010.

© 2026 by the author(s). Distributed under a Creative Commons CC BY license.

Preprints.org (www.preprints.org) | NOT PEER-REVIEWED | Posted: 1 April 2026 doi:10.20944/preprints202604.0022.v1

92. Amador, C.I.; Stannius, R.O.; Røder, H.L.; Burmølle, M. High-Throughput Screening Alternative to Crystal Violet Biofilm Assay Combining Fluorescence Quantification and Imaging. *Journal of Microbiological Methods* **2021**, *190*, 106343, doi:10.1016/j.mimet.2021.106343.
93. Stepanović, S.; Vuković, D.; Hola, V.; Bonaventura, G.D.; Djukić, S.; Ćirković, I.; Ruzicka, F. Quantification of Biofilm in Microtiter Plates: Overview of Testing Conditions and Practical Recommendations for Assessment of Biofilm Production by Staphylococci. *APMIS* **2007**, *115*, 891–899, doi:10.1111/j.1600-0463.2007.apm_630.x.
94. Zhou, C.; Ding, Z.; Guo, Q.; Jiang, M. Visualization of Antimicrobial-Induced Bacterial Membrane Disruption with a Bicolor AIEgen. *Chemosensors* **2022**, *10*, 284, doi:10.3390/chemosensors10070284.
95. Bucarey, S.A.; Pujol, M.; Poblete, J.; Nuñez, I.; Tapia, C.V.; Neira-Carrillo, A.; Martinez, J.; Bassa, O. Chitosan Microparticles Loaded with Yeast-Derived PCV2 Virus-like Particles Elicit Antigen-Specific Cellular Immune Response in Mice after Oral Administration. *Virol J* **2014**, *11*, 149, doi:10.1186/1743-422X-11-149.

Disclaimer/Publisher's Note: The statements, opinions and data contained in all publications are solely those of the individual author(s) and contributor(s) and not of MDPI and/or the editor(s). MDPI and/or the editor(s) disclaim responsibility for any injury to people or property resulting from any ideas, methods, instructions or products referred to in the content.

© 2026 by the author(s). Distributed under a Creative Commons CC BY license.